

Contents lists available at ScienceDirect

Journal of Sound and Vibration

journal homepage: www.elsevier.com/locate/jsvi

Aeroacoustics research in Europe: The CEAS-ASC report on 2008 highlights

D. Juvé *

Laboratoire de Mécanique des Fluides et d'Acoustique, UMR CNRS 5509, 36 Avenue Guy de Collongue, 69134 Ecully Cedex, France

ARTICLE INFO

Article history:

Accepted 16 July 2009

The peer review of this article was organized by C.L. Morfey

ABSTRACT

The Council of European Aerospace Societies (CEAS) Aeroacoustics Specialists Committee (ASC) supports and promotes the interests of the scientific and industrial aeroacoustics community on an European scale and European aeronautics activities internationally. In this context, "aeroacoustics" encompasses all aerospace acoustics and related areas. Each year the committee highlights some of the research and development projects in Europe.

This paper is a report on highlights of aeroacoustics research in Europe in 2008, compiled from information provided to the ASC of the CEAS.

During 2008, numerous research programmes were funded by the European Union. Some of the contributions submitted to the editor summarize selected findings from these programmes, while other articles cover issues supported by national associations or by industries. Furthermore, a concise summary of the workshop on "Turbomachinery Broadband Noise" held in Bilbao in October is included in this report.

Enquiries concerning all contributions should be addressed to the authors who are given at the end of each subsection.

© 2009 Elsevier Ltd. All rights reserved.

1. CEAS-ASC workshop

The 12th workshop of the CEAS Aeroacoustics Committee, devoted to "Turbomachinery Broadband Noise" was held in the Faculty of Engineering of Bilbao, Spain, on 23–24 October 2008. It was locally organized by Ana Villate, from the Aeronautical Technologies Centre (CTA). The chairman of the scientific committee was Emilio Campos from INTA (Instituto Nacional de Técnica Aeroespacial), who will act as Guest Editor of a special issue of the International Journal of Aeroacoustics dedicated to the workshop. Turbomachinery noise is still dominated by tones but fan broadband noise emerges now as a practical issue for aircraft noise reduction. The interest in this subject was demonstrated by the 68 attendants and the 21 papers presented over two days. There were three keynote lectures, the first one being "PROBAND: Improvement of Fan Broadband Noise Prediction: Experimental Investigation and Computational Modelling" given by Lars Enghardt from DLR. Lars Enghardt presented a summary of the recently finished European project PROBAND devoted to the understanding of the broadband noise generation mechanisms and to the development of prediction methods using conventional or advanced computational techniques. The second lecture was given by Stewart Glegg from Florida Atlantic University. Entitled "The Effect of Blade Thickness and Angle of Attack on Broadband Fan Noise", it gave a review of the prediction methodologies for rotor alone noise and rotor stator interaction noise with emphasis on broadband effects. The third invited talk "Using Phased Array Beamforming to Identify Broadband Noise Sources in a Turbofan Engine" was presented by

* Tel.: +33 472186012; fax: +33 472189143.

E-mail address: daniel.juve@ec-lyon.fr

Pieter Sijtsma from NLR, who discussed the technique of location of the prevailing noise sources by means of phased array beamforming inside an engine rig using a circular microphone array. Many of the contributions presented were based on small-scale laboratory fans, including ventilation fans for cars as well, and some papers dealt with a single blade or a cascade but most subjects of importance for turbomachinery noise were considered. One of the key issues was clearly identified as the characterization of turbulence. Some papers were concerned with specific noise sources, for example associated with tip leakage flow. A number of contributions addressed blade or vane self noise, many dealing with both measurement and prediction. Analytical models were discussed, for isolated airfoils and for the interaction of turbulence with a cascade. Among the various computational techniques presented, a new approach, called IDDES, deserves special attention; it is a non-zonal hybrid RANS/LES approach with LES wall modelling capabilities for the simulation of turbulent structures in the boundary layer. Some attention was given to the sound propagation in a duct with sheared flow, both theoretically and computationally and an experiment on the nonlinear interaction between a source and a fan was presented. Finally the issue of turbine broadband noise was also considered.

Written by Emilio Campos, camposae@inta.es, INTA, Spain.

2. European-funded projects

2.1. NACRE 6th FP Integrated Project

NACRE (New Aircraft Concepts Research) is a large scientific and technology upstream research collaboration project, with a budget of over 30 m euros, partly funded by the European Union. The NACRE consortium is composed of members of the complete aeronautical supply chain. Running from 2005 to 2009, the project aims at creating, developing, validating and integrating technologies that will enable novel concepts to emerge and provide for future aircraft to be assessed and potentially developed for improved environmental friendliness, passenger comfort and overall efficiency, including manufacturer and airlines' costs. The research on aeroacoustics in NACRE is gathered essentially under the umbrella of the so-called Pro-Green domain. One of the objectives of Pro-Green, which amounts to 50 percent of the whole project budget, is to achieve some shielding of the powerplant noise propagating to the ground during take-off and landing, be it advanced turbofan engines or open rotor systems, in order to reduce the community noise exposure in the vicinity of airports (Fig. 1). Multidisciplinary investigations on engine integration paved the way to a major wind-tunnel test campaign for the assessment of noise shielding. In particular, a realistic wind-tunnel model has been designed and manufactured, featuring noise source models that are representative of an engine system, enabling a suitable balance between an excellent representativeness and enough flexibility on the positioning of the noise sources, so that the investigation remains generic enough and not overly configuration-related. Computational models were extensively developed and applied to this advanced engine installation configuration. In parallel, the Pro-Green aircraft concepts feature a range of advanced wing concepts, high-aspect ratio low sweep turbulent designs or forward sweep laminar designs for various Mach numbers, where the aim is not simply to achieve fuel-efficient designs (through an aerodynamic and structure optimization) but also, given the very innovative designs, to address the challenge of systems integration and noise reduction for the airframe, including landing gear integration studies. The NACRE consortium, spearheaded by Airbus, is composed of 36 partners from 13 European countries (including Russia), providing an impressive spread of expertise and capability for this industry throughout the EU and constituting the complete aeronautical supply chain: Airbus, Alenia, Dassault Aviation, Piaggio Aero, Rolls-Royce, Snecma, MTU Aero Engines, Aircelle, Messier-Dowty, Dowty Propellers (GE), ARA, CIRA, DLR, EADS IW, FOI, INTA, NLR, ONERA, VZLU, TsAGI, Trinity College Dublin, University Greenwich, TU München, University Stuttgart, KTH, Warsaw University of Technology, ISVR, PEDECE, INASCO, IBK and ARTTIC.



Fig. 1. A sustainable low-noise open-rotor-powered Pro-Green aircraft concept.

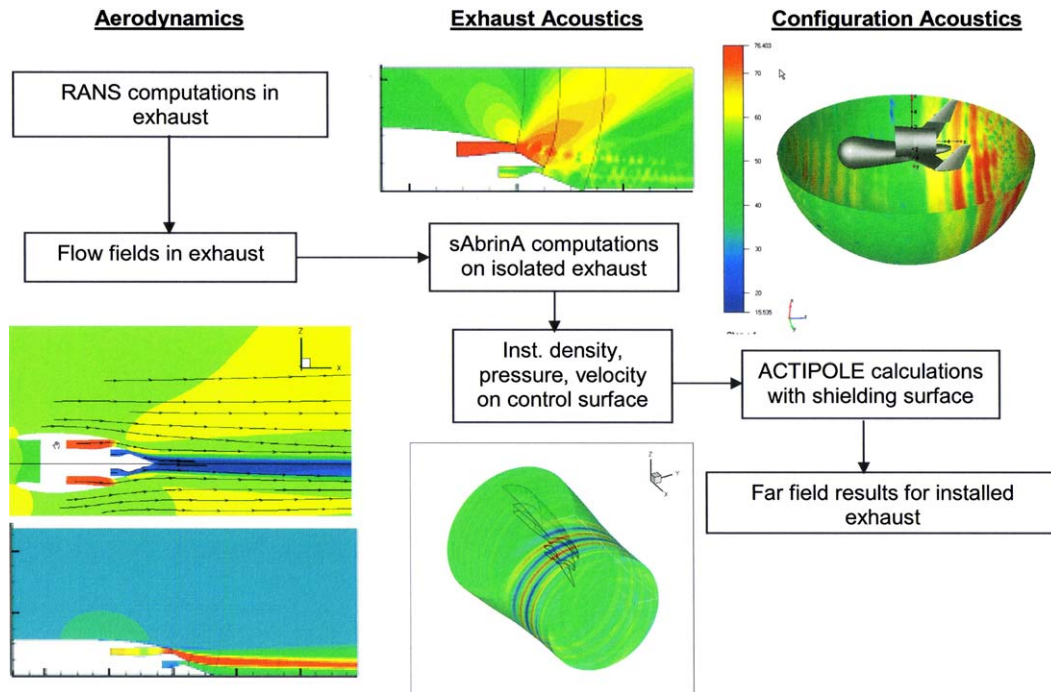


Fig. 2. Coupling of free-field and boundary-elements codes.

From both the experimental and computational work within NACRE, some highlights are presented below.
 Written by João Frota, joao.frota@airbus.com, Future Projects, Airbus, France.

2.1.1. Numerical simulation of turbofan noise shielding

Among the most promising concepts studied in NACRE, the “Rear Fuselage Nacelle—RFN” configuration based on mounting the engines at the rear fuselage above the empennage takes advantage of a non-negligible acoustical shielding effect by the airframe on the fan noise emission. In the context of the numerical simulation of installation effects of the RFN configuration, ONERA and Airbus have developed a hybrid method taking into account external uniform flow, associating ONERA’s sAbrinA FEE (Full Euler’s Equation) solver [1] and Airbus’ ACTIPOLE BEM (Boundary Elements Method) code developed by EADS-IW [2]. The different steps of the coupling process are described in Fig. 2. Several computations for different flight conditions have been performed with this coupling process. The methodology has been numerically validated on engine-alone configurations, comparing full ONERA’s sAbrinA free-field computations to sAbrinA/ACTIPOLE coupling results. The complete theoretical predictions of the expected shielding effects will then be validated against experimental data obtained during the NACRE Wind Tunnel Test campaign that took place in ONERA CeprA19 facility in November 2008.

Written by Céline Parzani, celine.parzani@airbus.com, Johanna Chappuis, johanna.chappuis@airbus.com, Airbus France, Guillaume Desquesnes, guillaume.desquesnes@onera.fr, Onera, France.

2.1.2. Numerical simulation of open rotor noise shielding

In recent years, the contra-rotating open rotor concept has received significant attention as it has the potential to increase propulsion efficiency substantially and therefore reduce engine emission compared to shrouded turbofan engines. Open rotors, however, are not expected to be as quiet as next-generation turbofans. To alleviate this problem, a Pro-Green aircraft concept, in which the noise generated by two aft-mounted open rotors is shielded by a U-tail, has been studied in NACRE. NLR has assessed the shielding effect for the low-frequency tones by solving the linearized Euler equations with the NLR ENFLOW CFD/CAA system. Multi-block structured grids are employed and the equations are discretized by a high-order finite-volume scheme with low numerical dispersion [3,4]. This scheme is fourth-order accurate, conservative, and dispersion-relation preserving on non-uniform, curvilinear grids. From the near-field solution, the far-field sound is computed using a Kirchhoff surface integral formulation. The near-field solution for a typical rotor tone at $kR = 6.95$ (R is rotor tip radius) is illustrated in Fig. 3. The far-field noise attenuation due to the shielding by the U-tail and fuselage is shown in Fig. 4. The blue region indicates the shadow region where effective shielding of 10–15 dB is obtained.

Written by Johan C. Kok, jkok@nlr.nl, NLR, The Netherlands.

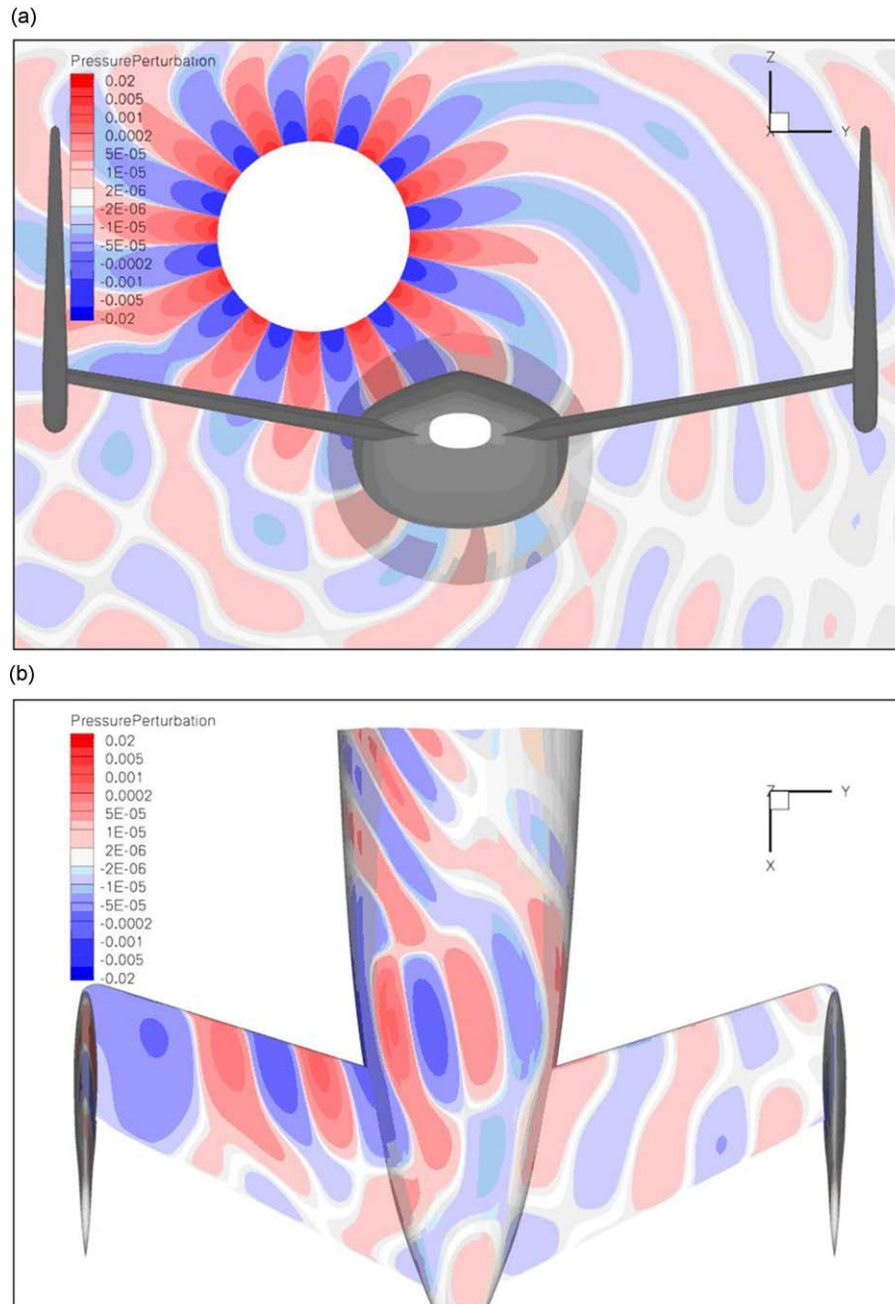


Fig. 3. Instantaneous pressure perturbation (scaled by ambient pressure) for Pro-Green aircraft concept with aft-mounted open rotor, full take-off power, $kR = 6.95$, left engine: (a) plane through engine center and (b) upper surface of configuration.

2.1.3. Wind tunnel tests on jet and fan noise shielding

Jet and fan noise are major contributors to airplane noise at take-off and landing. Within NACRE, unconventional engine integration concepts have been studied, in order to reduce those noise sources by using optimized shielding effects due to wing, empennage and fuselage surfaces. Two test campaigns were thus led at the CeprA19 acoustic test facility in Saclay—France [5,6]. The first one (2007) was dedicated to jet noise and the second one (2008) to fan noise. These test campaigns provided a significant database on shielding effects by simulating numerous configurations at several power settings in static and flight conditions. Other installation effects such as the impact of the pylon, of flap and slats, of primary and secondary chevrons were also studied so as to investigate all the possibilities to reduce noise through a noise-driven engine integration (Fig. 5). The results of the jet noise campaign show for example a substantial benefit due to the shielding effect of the wing for a large range of angles from 70° to 110° (with reference to jet axis). Fig. 6 shows the acoustic benefit

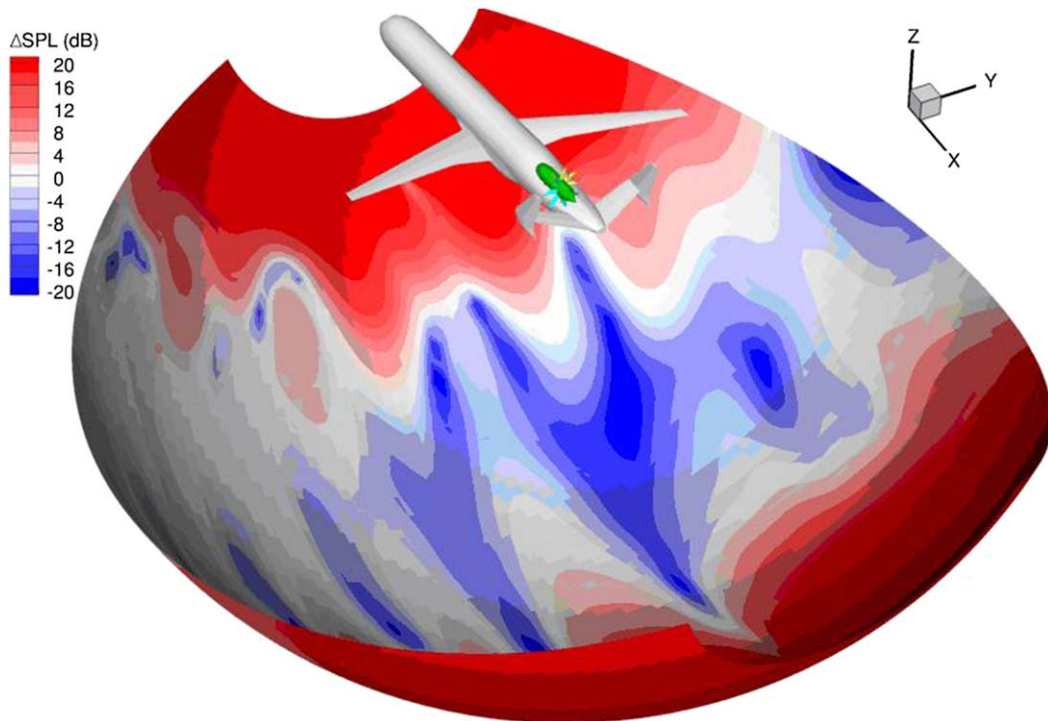


Fig. 4. Far-field noise attenuation at 46 m for Pro-Green aircraft concept with aft-mounted open rotor, full take-off power, $kR = 6.95$, left engine.

achieved on a jet noise simulator with primary and secondary chevrons in installed configuration compared to the isolated configuration for different power settings (CB: Cutback, SL: Sideline, HP: High Power) in flight conditions [5]. The results from the two acoustic campaigns are used to validate and calibrate analytical and numerical prediction tools developed in the frame of the NACRE project and in follow-up projects like CleanSky. These data will also be used as input for global aircraft performance assessment.

Written by Sébastien Aeberli, sebastien.aeberli@sneema.fr, Snecma, France.

2.2. TURNEX

In June 2008, the EU project TURNEX (Turbomachinery Noise Radiation through the Engine Exhaust) was completed. The goal of TURNEX was to develop concepts and enabling technologies for the reduction of engine noise at the source, through an improved understanding, modelling and prediction of fan and turbine noise radiation from exhaust nozzles, and through the evaluation of a number of low-noise exhaust nozzle configurations [7]. At its conclusion, TURNEX has delivered validated industry-exploitable methods for predicting turbomachinery noise radiation through exhaust nozzles. It has also delivered a technical assessment on the way forward for European fan noise testing facilities and an assessment of exhaust nozzle concepts for noise reduction at source. From both the experimental and modelling work within TURNEX, some highlights are presented below.

2.2.1. Large-scale rig test [8–11]

In the main experiment, two model scale exhaust nozzle configurations were tested in the QinetiQ Noise Test facility (NTF), using simulated fan and turbine noise sources and advanced measurement techniques. The rig included a rotating bypass duct section with wall-mounted microphones for radial mode analysis (RMA); Fig. 7 shows a detailed schematic of the test rig with the cowl (short cowl) assembly. A far-field azimuthal microphone array (FFA) was designed and installed, which could be moved over a range of axial positions and hence polar angles. This enabled 3D effects and the azimuthal mode content in the far field to be studied. An example of results obtained from the duct RMA (Fig. 8) demonstrates that the Mode Synthesiser worked well and generated the target modes with high tone protrusion.

2.2.2. Validation of CAA codes [12–15]

A key part of TURNEX was the validation of several prediction codes with the experimental data acquired in other tasks of the project. A typical result is shown in Fig. 9 which represents measured noise levels from the two different far-field arrays (“Polar” and “Azimuthal”) compared to predictions from the Actran/DGM and FLESTURN codes [14,15], using as the source input the mode amplitudes measured with the RMA. This is validation in both far-field level and directivity shape,

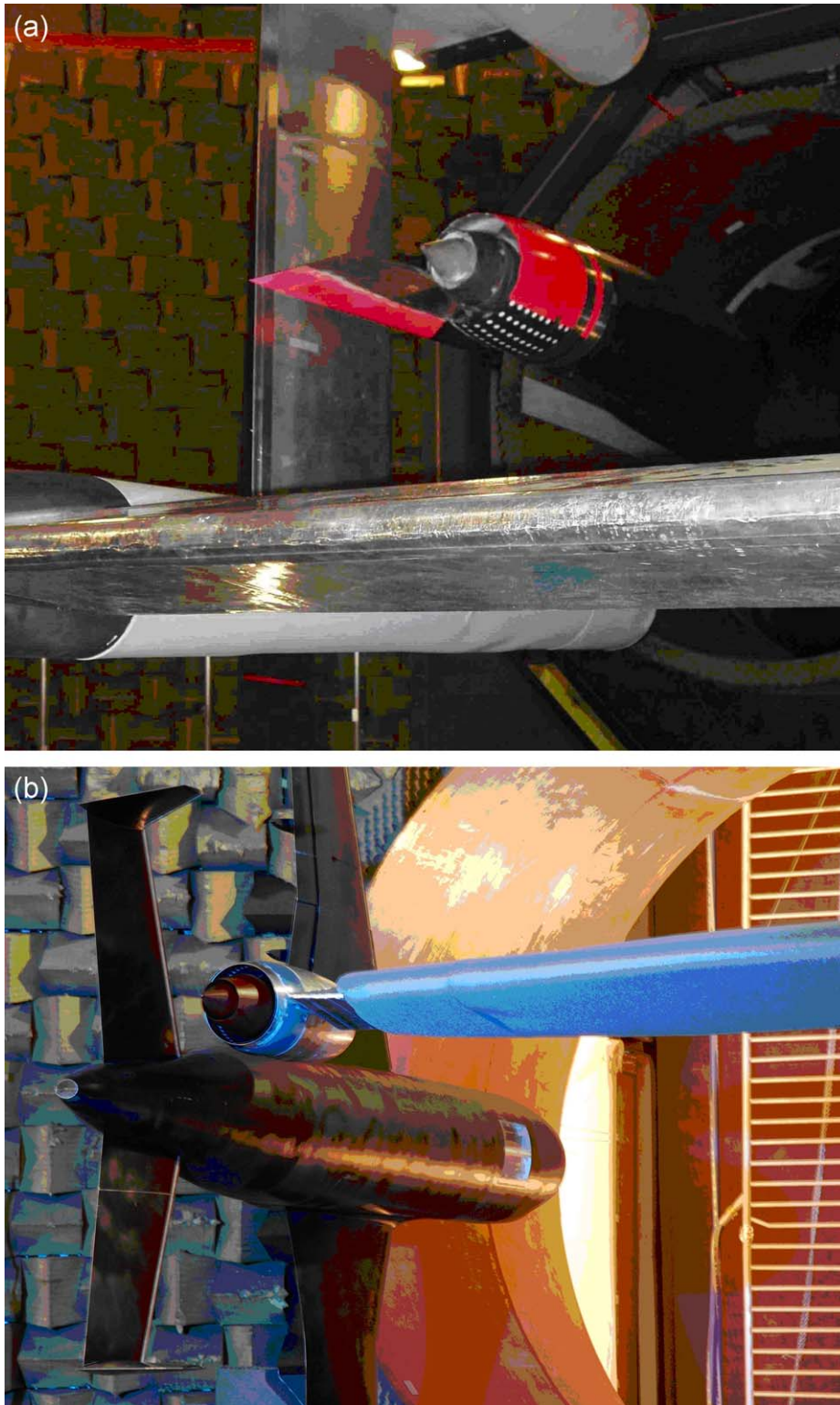


Fig. 5. NACRE wind tunnel tests in CeprA19: (a) jet noise simulator with pylon in over wing nacelle configuration and (b) fan noise simulator in rear fuselage configuration with complete aircraft.

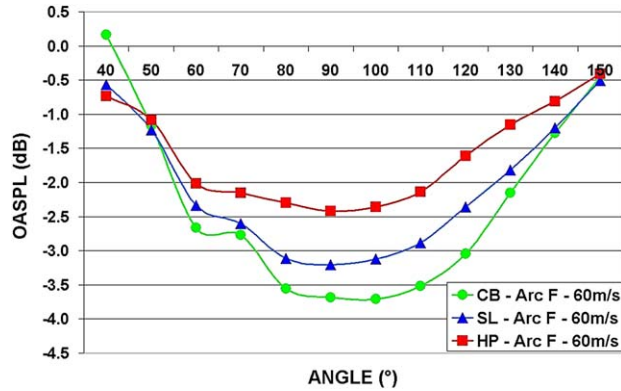


Fig. 6. Variation of OASPL between isolated and installed configuration in flight condition (CB: Cutback, SL: Sideline, HP: High power).

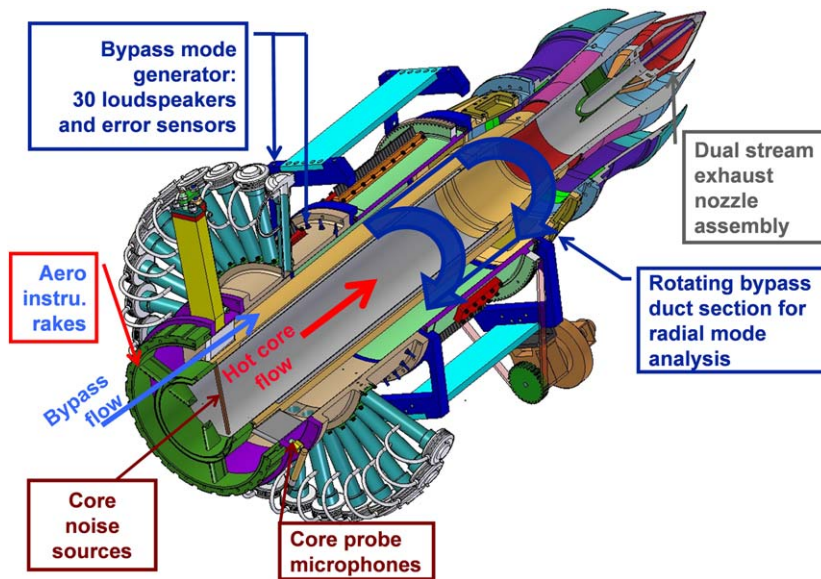


Fig. 7. Test rig with short cowl bypass nozzle installed, without pylon, showing bypass duct sound sources (“Mode Synthesiser”) and rotating microphone array for azimuthal and radial mode measurement.

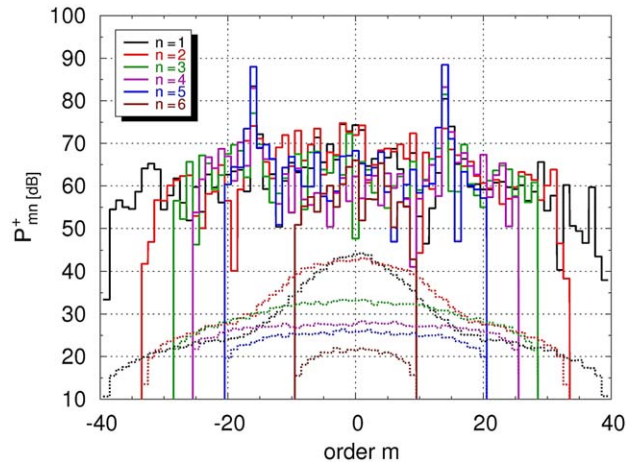


Fig. 8. Sound power azimuthal spectrum of radial modes propagating downstream measured in RMA duct section for target mode $mt = 14$ with associated spill over mode $m = -16$ at 14.4kHz at approach (solid lines: sound power P^+ ; dotted lines: standard deviation).

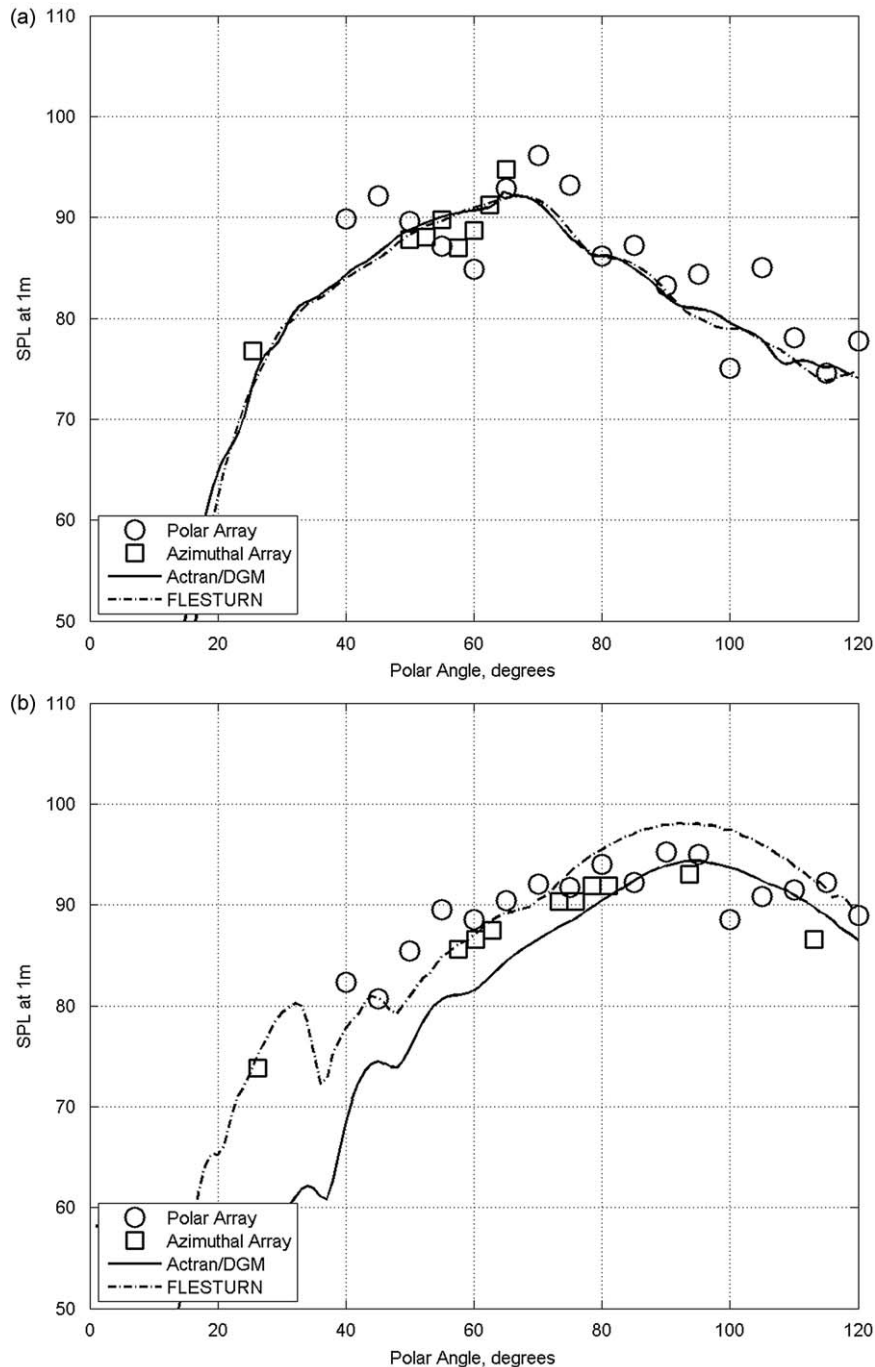


Fig. 9. Validation of CAA codes in TURNEX: (a) validation of Actran/DGM & FLESTURN, $\frac{3}{4}$ cowl at Approach, simulated fan BPF 8500 Hz, $m = 10$ and (b) validation of Actran/DGM (GTS) & FLESTURN, Long cowl at Cutback, simulated fan $\frac{1}{2}$ BPF, 5740 Hz, $m = 9$.

which is unusual in the context of aircraft noise prediction methods where normally the level is based on a semi-empirical “calibration” and only the directivity or field shape is usually validated.

2.2.3. Tone Haystacking

The above codes address propagation through the steady component of the exhaust jet flow(s). However, industry also requires methods for predicting the effects of scattering by the turbulent components within the jet shear layer(s), which leads to broadening or “haystacking” of high frequency turbine tones and also spatial scattering into azimuthal modes other than those excited initially by the turbine tone generation processes. TURNEX has made significant advances in this

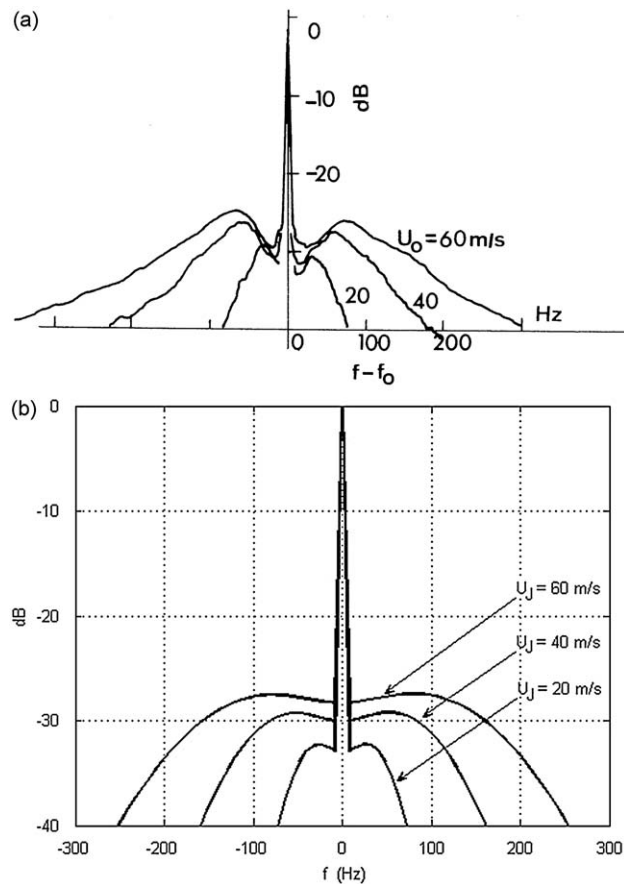


Fig. 10. Haystack spectra: (a) variation of measured spectra with velocity, from Candel [41], and (b) predicted spectra based on weak scattering Cargill method with frozen turbulence model.

subject by (1) evaluating an analytic, asymptotic solution based on the Cargill “weak” scattering method, which appears to be robust and can be rapidly computed [16] and (2) developing and evaluating the application of a time domain CAA code, PIANO, which does not suffer from the limitation of weak scattering. Both methods have been initially tested against published experimental data by Candel (Fig. 10a). The analytic model reproduced essentially the experimental trends with jet velocity and frequency (Fig. 10b), while the results of the DLR PIANO CAA code were in good quantitative agreement with the measurements obtained at different frequencies and velocities (see subsection 5.2 below). Measured data acquired under TURNEX are available for validation of these and other methods for more realistic jet flow conditions.

2.2.4. Jet shielding

Turbomachinery and other noise sources radiated from engines installed under the aircraft wing are partially reflected by the wing and then partially shielded by the coaxial jet exhaust flow before arriving at the observer position on the ground (Fig. 11). In TURNEX the shielding of noise by coaxial heated jets was studied with the aid of both asymptotic and numerical solutions (NLS) to the Lilley equation for steady refraction or shielding of sources outside the jet [17]. Comparisons between models and experimental data from the main TURNEX test have shown that the theories agree well with experiment, as illustrated in Fig. 12. From this study, it is recommended that, in general, NLS should be used if accurate shielding predictions are required at particular frequencies but if predictions are required at many frequencies, e.g. for broadband sources, a combination of the asymptotic methods offers a means to compute this quickly and with acceptable accuracy. At high frequencies the effects outside the cone of silence appear to be well predicted by the application of simple ray theory with a plug flow model of the jet. Inside the cone of silence the shielding becomes independent of the centerline Mach number and temperature, and can be accurately predicted by modelling the shielding as if it were caused by the reflection and diffraction by a “solid” body of radius equal to the jet nozzle, with a pressure release boundary. This is a key result and offers a means of implementing the shielding effect inside the cone of silence (where rays cannot penetrate).

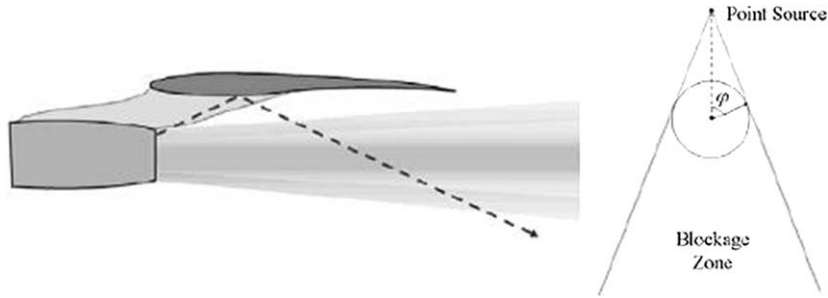


Fig. 11. Shielding of engine noise sources by co-axial jet flow.

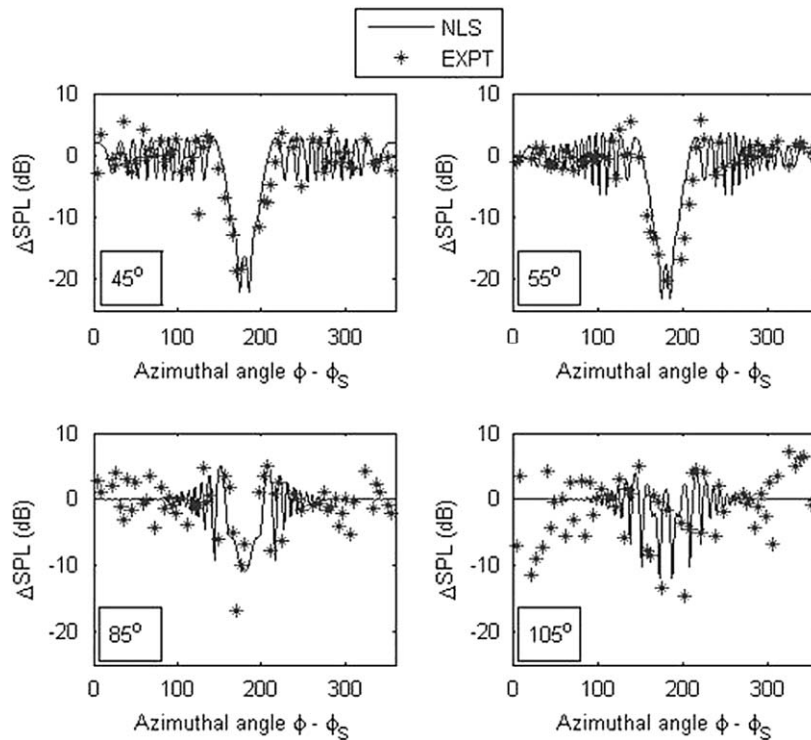


Fig. 12. Comparison of numerical (continuous line) results (NLS) with experimental (symbols) from TURNEX model coaxial jet test, at approach. Polar angle θ is shown in the bottom left of each frame.

2.2.5. In-duct to far-field beamformer method for broadband noise

A method for estimating far-field broadband noise levels from in-duct measurements in the form of a beamformer technique has been evaluated with the aid of data acquired from the main TURNEX test. This is based on cross-spectrum measurements taken with a simple flush-mounted, in-duct axial array of microphones. In effect, an in-duct directivity is measured and a computed transfer function is used to project that directivity into the far-field, which should be insensitive to the source model assumed and this does appear to be the case, provided any influence on the directivity is taken into account, such as a change in duct area or refraction by the jet exhaust flow. The estimated far-field results with an angle correction included for the area change between the beamformer array and the bypass nozzle are compared with measured data in Fig. 13.

Written by B.J. Tester, brian.j.testers@dsl.pipex.com, ISVR, UK.

3. Airframe noise

3.1. Fuel vents and panel joints

The Marie Curie FP6 EST programme AeroTraNet (www.imft.fr/Aero-TraNet) is in its third year of its 2006–2009 work programme. This network of four universities and three industrial collaborators has been undertaking research in unsteady

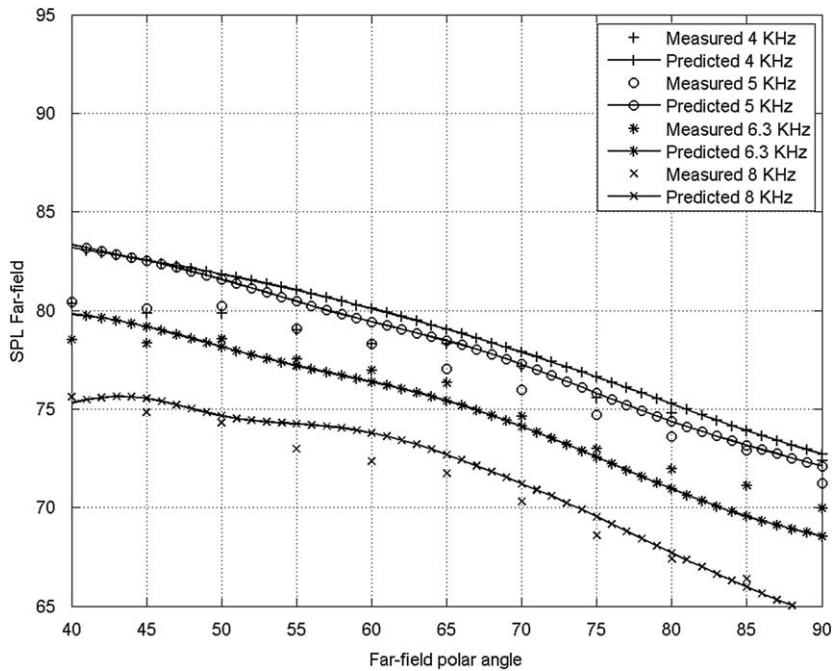


Fig. 13. Axial beamformer far-field broadband noise predictions compared to measured data, based on TURNEX rig data acquired at QinetiQ ($\frac{1}{3}$ octave band filtered data).

airframe cavity flow and noise. Work has focused on rectangular and cylindrical cavity flows, using experimental, numerical and flow control techniques. Rectangular cavities with a thick boundary layer were found to exhibit no Rossiter-type instability. Particle image velocimetry has shown the breakdown of the incoming boundary layer streak structure across the opening, leading to a broadband dominant incoherent motion in which a low-frequency shear layer flapping mode is enhanced [18]. At this regime, relevant to airframe panel lap joints and automobile door seals, broadband noise suppression concepts are required. Reducing the inflow boundary layer momentum thickness to cavity length ratio below $\frac{1}{30}$ enables the onset of tonal instabilities. Tomographic PIV has shown these tones including their spanwise coherence, which is required to correctly scale the far-field noise amplitude by acoustic analogy. Also, the high Reynolds number flow past a cylindrical cavity has been studied as a simplified model of the airframe fuel vent. Time-resolved CFD [19] and wind tunnel measurements show a shear layer flapping type tonal instability, with shoulder vortices and a very active cavity mid-span flow that produces noise. The sound directivity from this geometry is significant in the streamwise plane whilst a more uniform far-field radiation is predicted in the spanwise plane.

Written by Aldo Rona, ar45@leicester.ac.uk, University of Leicester, UK.

3.2. Direct simulations of airfoil noise

Airfoil self noise is a major noise source for many engineering applications such as airframes, wind turbines, fan blades, etc. Amiet (1976) provides a trailing edge (TE) noise theory, which uses only a frozen surface pressure spectrum as input to predict the far-field noise. A series of direct numerical simulations (DNS) have been conducted to investigate the noise generation by trailing edges and to evaluate Amiet's theory. The far-field noise obtained from a DNS of turbulent flow over an infinitely thin flat-plate trailing edge [20], intended to reproduce Amiet's assumption of a semi-infinite, zero thickness airfoil, showed good agreement with the theory. It was shown that a modified 2D theory produced satisfactory results for low frequencies, due to a strong spanwise coherence of the radiated sound at these frequencies (Fig. 14a). Two-dimensional DNS of airfoils with forced instability waves on the suction side revealed an unexpected phase shift between the incident and the scattered pressure fields for thick airfoils (or large wedge angles at the TE), such as NACA-0012 [21]. This was explained by the co-existence of two distinct frequencies, one associated with the wake and one with the instability wave convecting over the airfoil. This is in contrast to thinner airfoils, where the wake frequency locks into the frequency of the instability wave. Three-dimensional DNS of airfoils at $M = 0.4$ and $Re = 50,000$, originally designed to study laminar separation bubbles, indicated that significant additional noise sources are present, most of them located in the vicinity of the laminar-turbulent transition and turbulent reattachment region (Fig. 14b).

Written by Richard Sandberg, sandberg@soton.ac.uk, University of Southampton, UK.

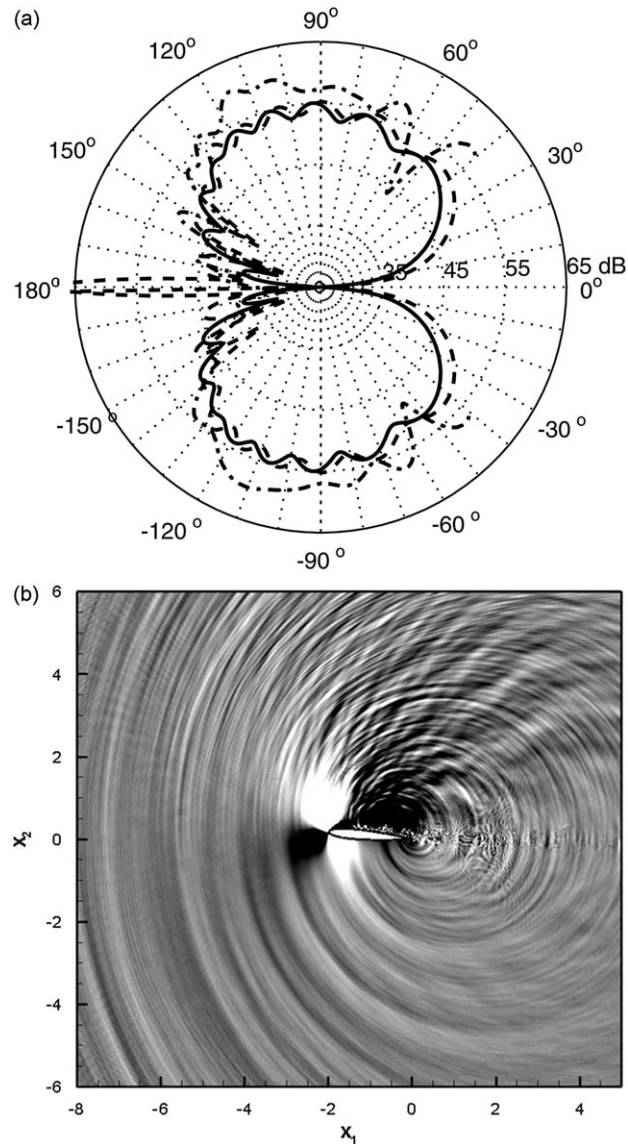


Fig. 14. Direct numerical simulation of airfoil noise (flat plate trailing edge) (a): magnitude of acoustic pressure in dB for reduced frequency $\mu_0 = 16.2$ using: — 3D acoustic analogy, - - - 2D acoustic analogy, . . . DNS, and (b) contours of dilatation for NACA-0012 airfoil at $M = 0.4$, $Re = 50,000$; angle of incidence $\alpha = 5^\circ$.

3.3. Wall-pressure fluctuations induced by attached and separated boundary-layers

The research group of the Mechanical Engineering Department of the University of Roma 3 carried out several experiments to study wall pressure fluctuations statistics and their connection to the flow structures in a variety of configurations of engineering interest. As an example, simultaneous PIV and wall pressure measurements have been conducted to characterize turbulent boundary layers crossing a forward-facing step. This experiment was conducted in collaboration with INSEAN (Italian Ship Model Basin research center). The overall statistics, including 2D velocity/pressure correlations, have been investigated in depth, allowing the role of the recirculation bubbles to be clarified [22]. Further studies have been conducted in collaboration with the Ecole Centrale de Lyon (Centre Acoustique, LMFA) on attached turbulent boundary layers with pressure gradients. A novel post-processing technique based on the computation of the cross-wavelet transform has been introduced [23]. The method has been used as a base for developing novel signal conditioning and ensemble averaging procedures.

Written by R. Camussi, camussi@uniroma3.it, Università Roma Tre, Italy.

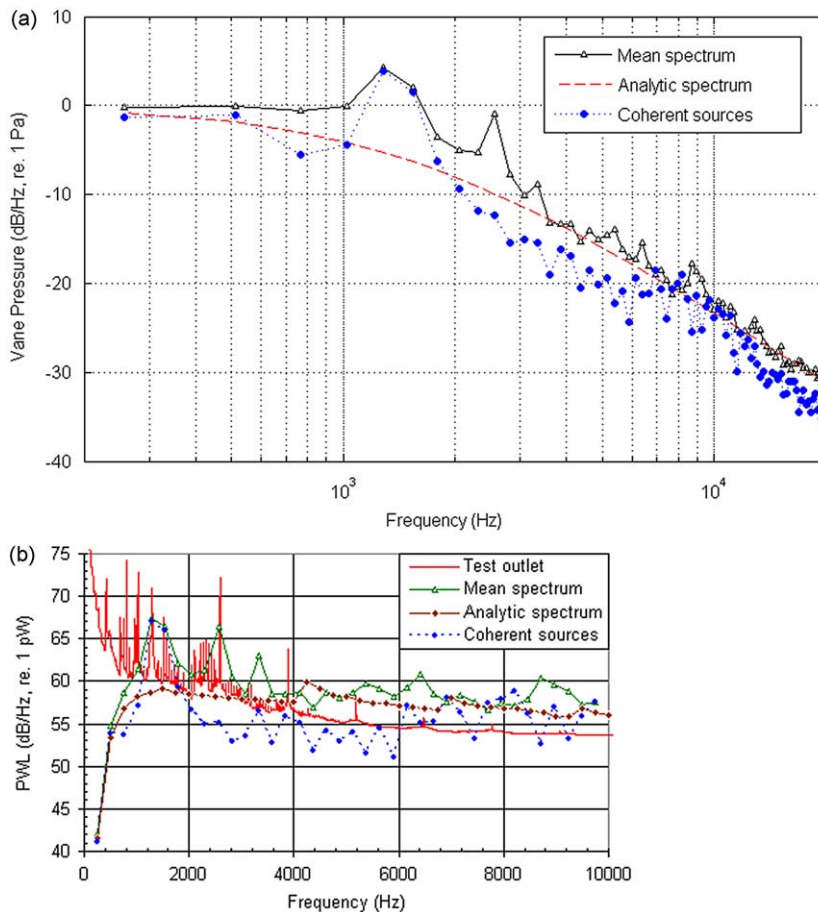


Fig. 15. Prediction of rotor-stator broadband noise using LES data and a simplified Green's function in the Ffowcs-Williams/Hawkings approach: (a) averaged vane pressure spectra deduced from LES outputs and (b) spectra of sound power level, PWL, radiated in the outlet duct.

4. Fan and jet noise

4.1. Prediction of rotor-stator broadband noise

Turbofan broadband noise is one of the main acoustic sources in high bypass ratio aircraft engines due to past reductions of jet noise and fan tone noise. Its prediction has thus become a new challenge for further progress. This is the objective of the European project PROBAND (2005–2008). ONERA proposed in this framework a numerical computation to be compared to tests in the DLR low speed axial fan in Berlin. A LES model, implemented into the ONERA code elsA, gives the random pressure fluctuations on the outlet guide vanes. These data are the inputs of an acoustic code based on the Ffowcs Williams and Hawkings equation for broadband fixed or rotating dipoles, the free-field Green's function being replaced by Green's function in a hard-walled cylindrical duct with a uniform mean flow. The acoustic free field is deduced from a Kirchhoff integral on the duct exit cross-section [24]. Signal processing of the vane pressure fluctuations leads to three possible spectra (Fig. 15a): (i) the mean spectrum on a vane chord; (ii) the least squares fitting the analytical curve $S(f) = -20 \log[C + (f/f_0)^\alpha]$ where $C = 1$, $\alpha = 1.36$, and $f_0 = 1467$ Hz; (iii) the spectrum taking into account the coherence along the chord (calculated after addition of time signatures along the chord). These three spectra are used to compute the sound power spectrum in the outlet duct where comparison with DLR test data is available (Fig. 15b). There is a strong underestimation at low frequencies, but the broadband level measured in this range could be due to secondary flows (separated flow in the hub region) which are ignored in the present aerodynamic simulation. On the contrary, prediction based on mean or analytic vane spectrum is too high by about 3–5 dB at high frequencies, probably because these spectra are calculated as if sources were compact along the chord. Finally, the assumption of coherent sources seems to lead to the best results, at ± 3 dB from the test [25].

Written by S. Léwy, Serge.Lewy@onera.fr, ONERA, France.

4.2. Numerical method for LEE applied to turbomachinery noise

A numerical method for the prediction of propagation and radiation of turbo-machinery noise has been developed [26,27]. For the near field, the method is based on the solution of the axisymmetric linearized Euler equations (LEE) in the frequency domain: for each wavenumber, an associated linearized Euler problem is solved using a finite element technique. This approach is particularly useful for design optimization calculations of the tonal noise generated by the turbine and fan. To reduce computational time and memory requirements, pressure gradients in the momentum equations are neglected. A similar approximation, called gradient terms suppression (GTS), is often used to overcome instability problems that prevent convergence of time domain LEE algorithms. While the GTS approximation suppresses all mean flow gradient terms, in the present case only the terms in momentum equations which involve density fluctuations are neglected. This allows to decouple the continuity equation and to solve only momentum and energy equations. A PML boundary formulation is used for the far-field and inlet boundaries. The numerical code can deal with structured and unstructured grids of both triangular and quadrilateral elements. The acoustic near field is then radiated in the far field using the formulation of Ffowcs Williams and Hawkins. Code validation was done by reference to the Munt problem. After validation the propagation of an imposed duct mode in a more realistic engine geometry was studied. The near-field

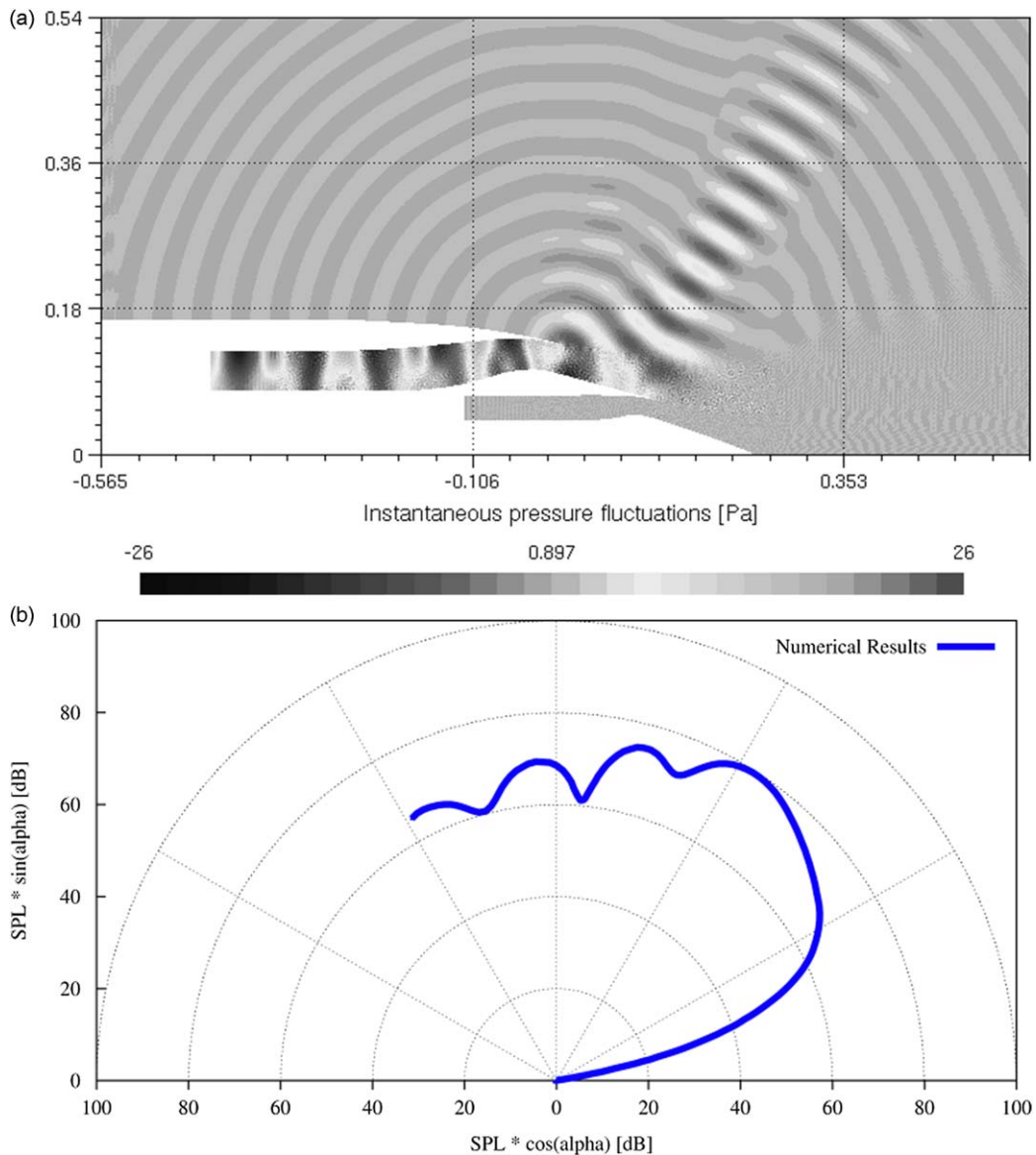


Fig. 16. Turbofan broadband noise: (a) turbofan geometry and snapshot of near-field instantaneous pressure fluctuations and (b) far-field directivity computed at a distance $r = 12$ m (mode (9,1), $f = 8282$ Hz, static approach condition).

instantaneous pressure perturbations for the duct mode (0, 1) in the static approach condition, with frequency 8282 Hz, is shown in Fig. 16a; in Fig. 16b, the corresponding sound pressure level (SPL) directivity pattern, describing the field radiated out of the engine at $r = 12$ m, is reported.

Written by R. Arina, renzo.arina@polito.it, A. Iob, andrea.iob@polito.it, Politecnico di Torino, Italy.

4.3. Numerical analysis of turbulent coaxial jet noise

In recent studies on turbulent jet noise [28,29], which encompass the acoustic effects of heat transfer across the shear layer, a hybrid large-eddy simulation/computational aeroacoustics (LES/CAA) approach is applied to determine the acoustic field. The source terms in the CAA formulation are related to certain noise generation mechanisms and thus, it is possible to analyze the acoustic sources in great detail. Using the noise source terms of the acoustic perturbation equations (APE) for a compressible source formulation (APE-4 system, [30]) the source strength inside hot coaxial jets is analyzed by a spectral decomposition. The acoustic results determined by the APE-4 system are presented in Fig. 17, where $D (= 2R)$ is the nozzle diameter and θ is the angular coordinate between the jet axis (z -coordinate) and the position vector from the nozzle exit. These results demonstrate that the acoustic radiation of coaxial jets can be strongly intensified by the pronounced temperature gradients.

Written by S.R. Koh, s.koh@aia.rwth-aachen.de, W. Schröder, M. Meinke, Institute of Aerodynamics RWTH, Aachen, Germany.

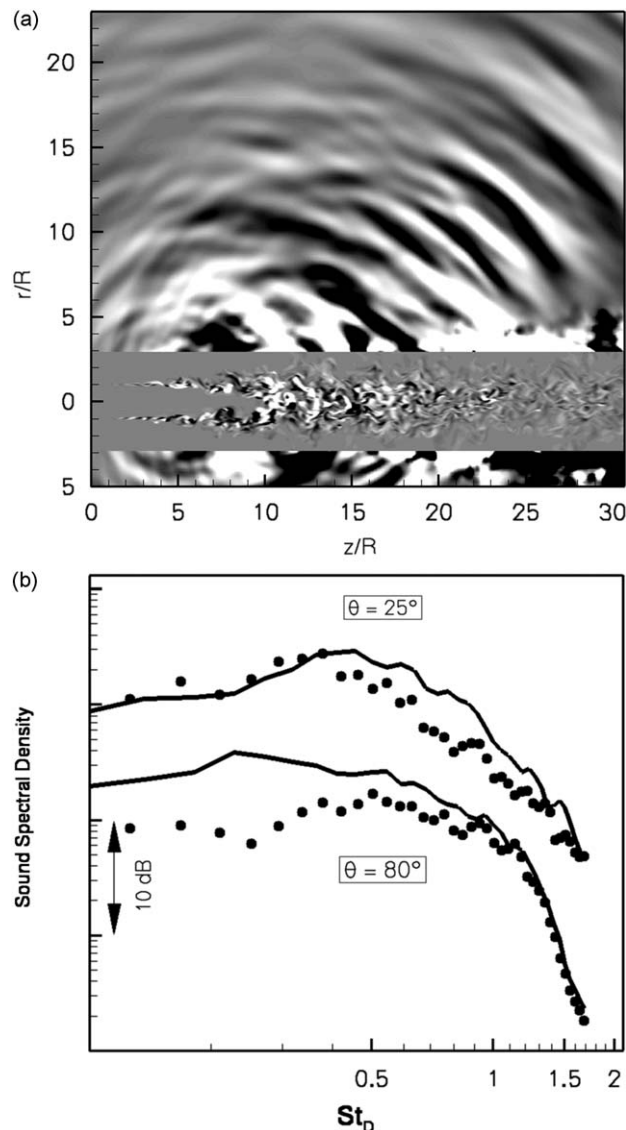


Fig. 17. Computation of hot coaxial jet noise by the APE-4 system: (a) snapshot of the noise source (for $r < 1.5D$) and of the acoustic pressure (for $r > 1.5D$) and (b) sound spectra versus Strouhal number, estimated at $20D$ (— hot jet; ... cold jet).

4.4. Jet noise modelling based on a generalized acoustic analogy informed by large eddy simulations

A hybrid prediction methodology for jet noise has been developed by the Universities of Cambridge and Loughborough [31]. The approach is a hybrid one made up of three components, with each component using modelling and numerical techniques optimized to suit a particular purpose. The propagation of noise to the far field is captured via a solution of the adjoint linearized Euler equations (LEE) to determine the adjoint Green function describing how sound emitted by the jet is modified by propagation through the time-averaged but spatially developing jet flow field and scattered by the rigid surfaces of the nozzle. The sound generation is described by Goldstein's acoustic analogy [32]. A Gaussian function is used to model the cross-correlation of the fourth-order velocity fluctuations which are the main acoustic sources in an isothermal jet. Parameters describing the source statistics (amplitude, length and time scales) are determined via a RANS calculation, where the remaining constants of proportionality were determined through comparison with correlations obtained from a large eddy simulation (LES). Comparison has also been made with an experiment at different Reynolds numbers and the constants appear to be universal. Thus informed by the LES solution, the source description is determined with no empirical constants and so leads to an absolute prediction for the far-field sound. This was compared with data for an experimental jet [33] and found to give excellent agreement across a wide spectral range and for both sideline and peak noise angles (Fig. 18).

Written by Ann Dowling, ann.dowling@eng.cam.ac.uk, University of Cambridge, UK.

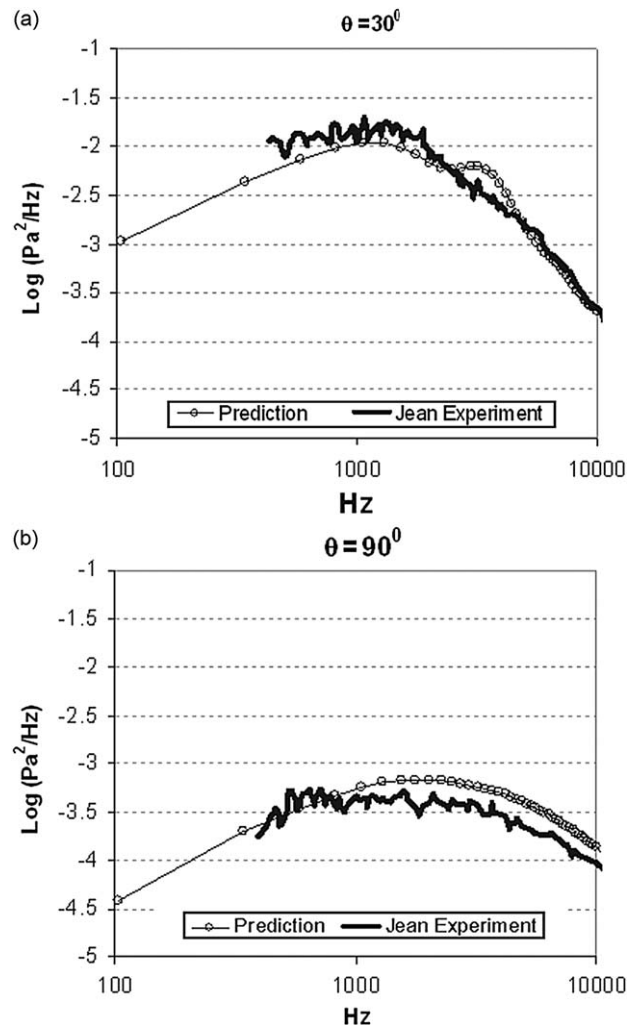


Fig. 18. Computed jet noise compared to experimental data: (a) at 30° to the jet axis and (b) at 90° to the jet axis. The predictions are based on a Green function for a spreading jet mean flow and a Gaussian source model informed by large eddy simulations.

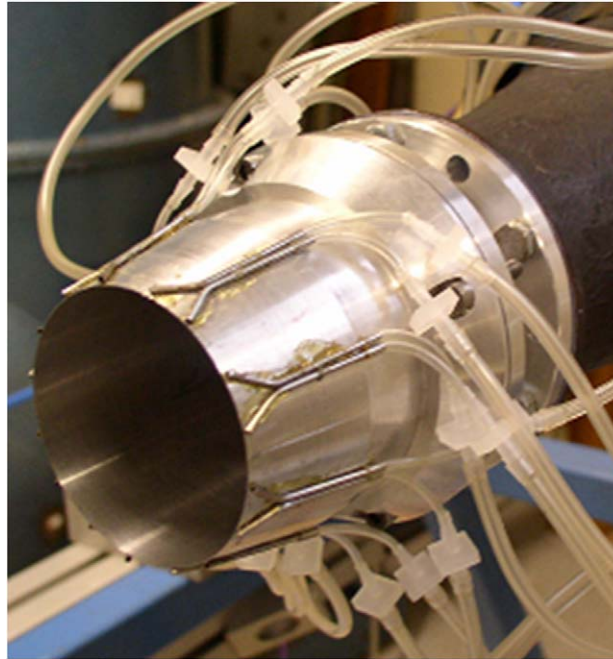


Fig. 19. Test model for jet noise reduction by fluidic injection.

4.5. Jet noise reduction by fluidic injection

A device for the reduction of jet noise was developed and studied [34]. The actuator consists of azimuthally distributed pairs of control jets which both penetrate the main jet and converge on one another (Fig. 19). The device produces an acoustic effect which is similar to that produced by non-converging control jets: far field sound levels are reduced over a frequency range $0 < St < 4$, this reduction is omnidirectional and sound levels are increased at higher frequencies. In the near-nozzle region, where the jet pairs interact with the main jet, the principal mechanism comprises an ejection between two jets of a pair; a local co-flow is thus produced, and the resulting reduction in mean shear leads to a strong local decrease (of the order of 70 percent) of turbulence production. This mechanism appears to be very different from that produced by non-converging microjets, where longitudinal vorticity is often cited as the mechanism which underpins the control effect. In the region between two pairs of control jets the turbulence characteristics remain almost identical to those of the uncontrolled flow. The azimuthal inhomogeneity produced by the device is dissipated within two jet diameters, after which the controlled flow recovers an axisymmetry very similar to that of the uncontrolled flow, but with turbulence levels globally reduced by about 10 percent, a potential core which is 10 percent longer, and a radial integral length scale which has been significantly reduced. In the context of an acoustic analogy it is the combined effect of the spatial correlation and the local turbulence intensity which is most pertinent for explaining the observed reduction of the radiated sound power.

Written by Yves Gervais, yves.gervais@lea.univ-poitiers.fr, Peter Jordan, LEA Poitiers, France.

4.6. Hybrid empirical methods for rocket noise modelling

In the framework of the project CAST funded by the Italian Space Agency, sound pressure levels around the VEGA launch system have been computed by means of a standard empirical model developed by Eldred [35] at NASA, and by means of a novel hybrid empirical/CAA approach [36]. The same jet sources employed in the empirical prediction are used to convolute a database of tailored Green's function computed by means of the frequency-domain CAA code GFD. Multi-frequency computations are carried out by exploiting the "immersed boundary" functionality of GFD in order to automatically generate the mesh around the VEGA launcher and its launch pad. Fig. 20a shows a comparison between the experimental SPL spectra measured at the launcher fairing level on the launcher surface and at a close location in the free-field, and the hybrid empirical/CAA results. The peak frequency is quite well predicted and the level difference between the fairing and free-field microphones increases with frequency, as observed experimentally. Although the hybrid empirical/CAA method is based on the same source distribution employed by the empirical model, these features are not observed in the purely empirical results plotted in Fig. 20b, since the empirical model does not take into account the noise diffraction effects due to solid obstacles. Moreover, the empirical model tends to underestimate the maximum noise frequency.

Written by M. Barbarino, m.barbarino@cira.it, D. Casalino, CIRA, Italy.

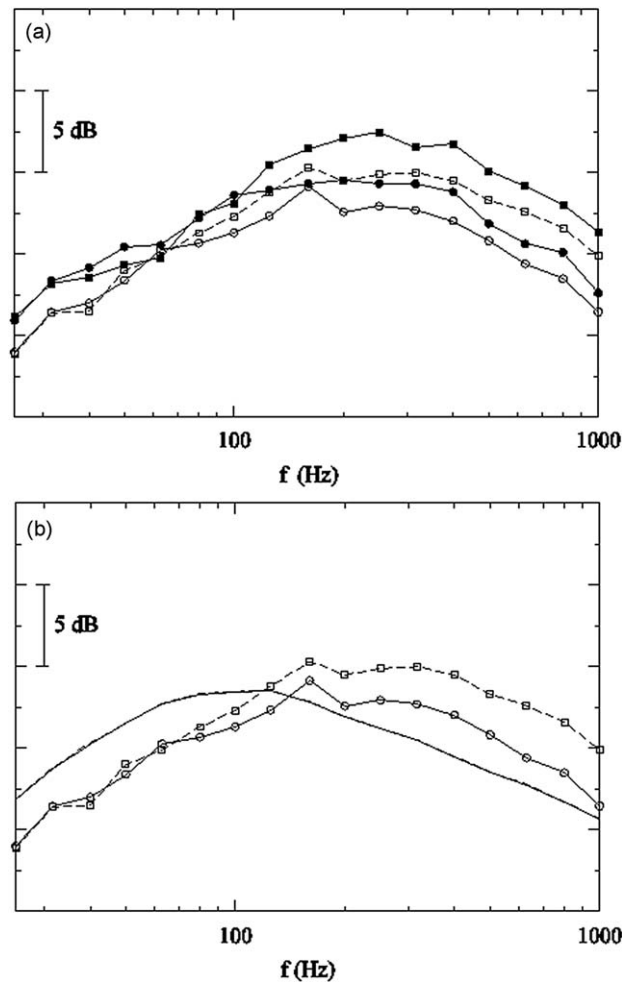


Fig. 20. Modelling of rocket noise spectra: (a) comparison between experimental data (open symbols) and hybrid empirical/CAA predictions (filled symbols) and (b) comparison between experimental data (open symbols) and fully empirical predictions (continuous line).

5. Techniques and methods in aeroacoustics

5.1. Development of a shock-capturing method based on adaptive spatial filtering for computational aeroacoustics

A shock-capturing method has been developed for nonlinear noise computations using low-dissipation schemes and centered finite differences [37]. It consists in applying an adaptive second-order conservative filtering in combination with a background selective filtering removing grid-to-grid oscillations. The magnitude of the shock-capturing filtering is determined dynamically from the flow solutions. A shock-detection procedure based on a Jameson-like shock sensor is derived so as to apply the shock-capturing filtering only around shocks. It allows to distinguish shocks from linear waves and from vortices when it is performed on the dilatation field. A second-order filter with reduced errors in the Fourier space with respect to the standard second-order filter is also designed. Linear and nonlinear test cases have been successfully solved to validate the shock-capturing method. Illustrations are provided in Fig. 21 for a problem of shock-vortex interaction [38]. Strong and multistage interactions with a regular reflection pattern are properly calculated. Finally the method is simple to implement and reasonable in terms of computational cost.

Written by C. Bogey, christophe.bogey@ec-lyon.fr, LMFA, UMR CNRS 5509, Ecole Centrale de Lyon, France.

5.2. The simulation of weak and strong haystacking with a CAA approach

The spectral broadening or haystacking effect is observed for tones propagating through a shear layer, causing a reduction of the tone peak in favor of a more distributed spectral hump around the tone frequency. In the weak scattering problem, the tone is still present as a prominent peak in the broadband spectrum. The strong haystacking effect is characterized by the complete absorption of the tone in the spectral hump. Strong haystacking for instance is observed in

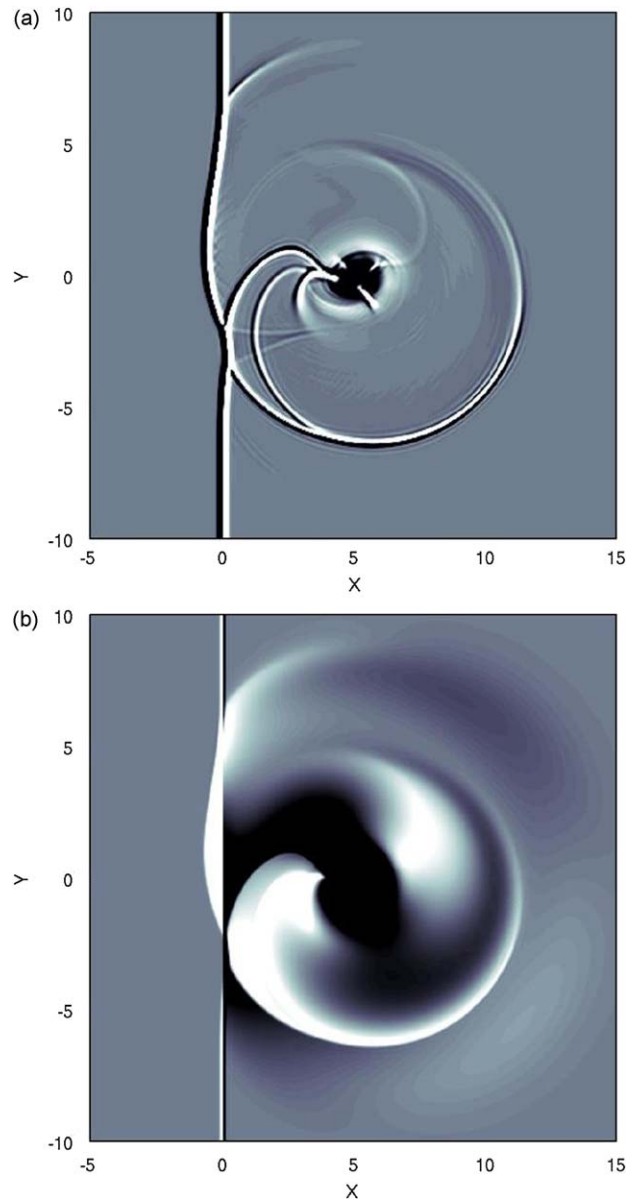


Fig. 21. Interactions between a planar shock wave (Mach number $M_s = 1.2$) and a Taylor vortex (maximum Mach number $M_v = 0.8$): (a) Laplacian of density and (b) fluctuating pressure.

experiments for propeller tones propagating through the shear layers of open wind tunnel sections. Within the European project TURNEX a CAA method was developed that enables the simulation of both the weak and the strong haystacking effects [39]. We simulate haystacking by solving the LEE with the CAA code PIANO of DLR, replacing the usual steady mean-flow with an unsteady turbulent base flow. The latter is generated by superposing a steady RANS mean-flow solution with synthetic turbulence. The recently developed random particle mesh (RPM) method of DLR is applied to generate 4D synthetic turbulence with all essential physical characteristics [40]. For the validation of the prediction the experiment of Candel et al. [41] is used, where spectral broadening was studied placing a sound source on the axis of a circular unheated jet. The general shape of the haystack predicted by CAA is in close agreement with the experimental findings. Further on, the effects of the variations in speed, shear layer thickness, and frequency on spectral shape are very well reproduced with CAA. For example, Fig. 22 shows a direct comparison of prediction and measurement of the haystack spectrum for three source frequencies at 60 m/s jet velocity and an axial position corresponding to 0.3 m shear layer thickness. The frequency shift of the spectral humps is well captured.

Written by R. Ewert, O. Kornow, T. Röber, J.W. Delfs, German Aero-space Center (DLR), M. Rose, Rolls-Royce Deutschland, Germany.

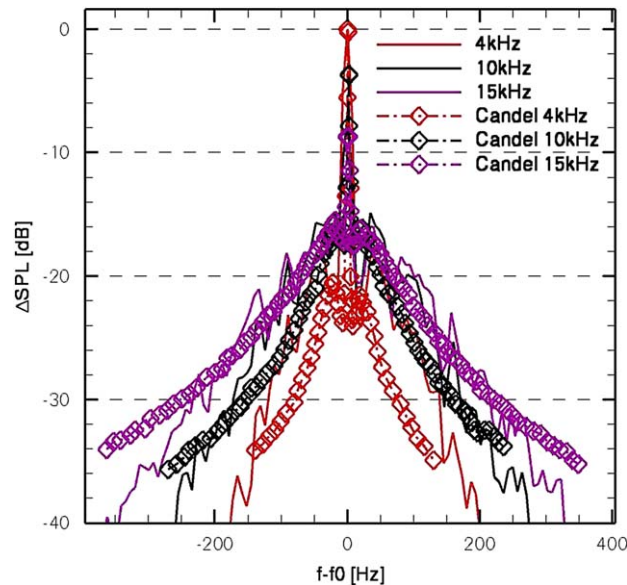


Fig. 22. Comparison of a stochastic CAA haystacking model (RPM) with measured haystack spectra (Candel et al.) for three source frequencies.

5.3. Curved boundary treatment for the discontinuous Galerkin method

In order to model the aeroacoustic noise propagation in non-quiet media, described by the linearized Euler equations, discontinuous Galerkin methods (DGM) on unstructured grids have been shown to be successful for complex geometries [42]. Special care is needed when formulating the boundary conditions at curved walls. A linear treatment of the geometry can limit the accuracy at high order [43]. For this reason, two different high-order boundary treatments, based on a quadratic representation of the geometry, are investigated. The first (mixed) treatment retains the quadrature-free discontinuous Galerkin implementation on elements with straight edges, while using (opposite to the classical “linear treatment”) the curved geometry normals to prescribe the boundary condition on velocity. The second (quadratical) treatment results from the formulation of the DGM on boundary elements that are conform to the shape of the curved geometry, locally requiring quadrature. As shown in Fig. 23 for the sound scattering over a 2D cylinder, the “mixed” treatment results in a slight improvement, but does not reduce the local phase error. This error is eliminated by the full quadratic treatment. The latter requires more memory storage because of its incompatibility with the quadrature-free technique, but the total overhead is not prohibitive, as such elements only exist in the vicinity of curved wall boundaries. The use of highly curved elements in conjunction with explicit time integration schemes raises stability issues that lead to reduced time steps. However, if high accuracy is needed, the full quadratic treatment is necessary to take advantage of the arbitrary order featured by DGM, without the burden of re-meshing.

Written by T. Toulorge, thomas.toulorge@mech.kuleuven.be, W. De Roeck, W. Desmet, Katholieke Universiteit Leuven, Belgium.

5.4. Application of Amiet’s theory in spanwise-varying flow conditions

Amiet’s theory, especially developed for thin airfoils in uniform flow, low angle of attack and without camber, is able to predict the airfoil sound radiation at high frequency, taking non-compactness effects into account in an explicit way. The airfoil lift response induced by an oblique gust impacting on an infinite span airfoil is obtained by a successive leading and trailing edge correction procedure from an initial solution. The far-field sound is then obtained from the pressure distribution on the airfoil with the help of a radiating dipole formulation in the convected free field. The main restriction of this theory is due to the assumed uniform upstream flow conditions along the airfoil span. In several industrial applications, as in wind turbines, fans, helicopter rotors or airfoils in jets, the properties of the flow (velocity, turbulence intensity, integral length scale of turbulence) are not constant along the span, and a modification of the theory is needed. To deal with spanwise-varying flow conditions, it is proposed to modify Amiet’s theory with a “Strip Method”: the complete airfoil is cut in a number of strips, having each their own upstream flow conditions. The overall noise radiated is then the summation of the noise emitted by each strip. However, the application of this direct strip method is not able to predict correctly the far-field noise. This is due mainly to the limited size of the strips that determines a maximum wavelength that can be captured. A new inverse strip method (Fig. 24a) is proposed to counter this problem by using a combination of large span airfoils [44]. The inverse method has been tested for several flow parameters and has shown its potential to reproduce correctly the radiated noise. For example, in the case of jet-airfoil interaction noise a maximum deviation of 5 dB in the range 500–10,000 Hz has been obtained (Fig. 24b).

Written by J. Christophe, christju@vki.ac.be, J. Anthoine, von Karman Institute for Fluid Dynamics, Belgium.

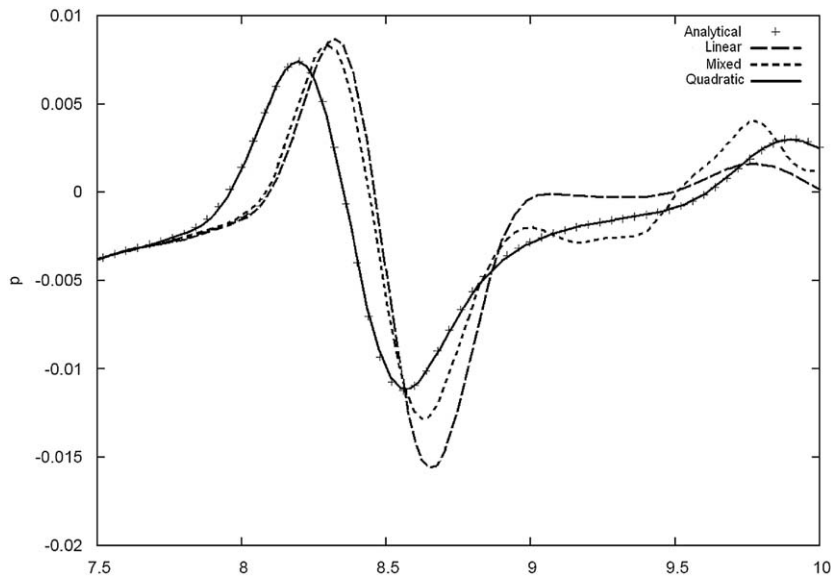


Fig. 23. Comparison of different curved boundary formulations for discontinuous Galerkin method applied to the sound scattering by a cylinder.

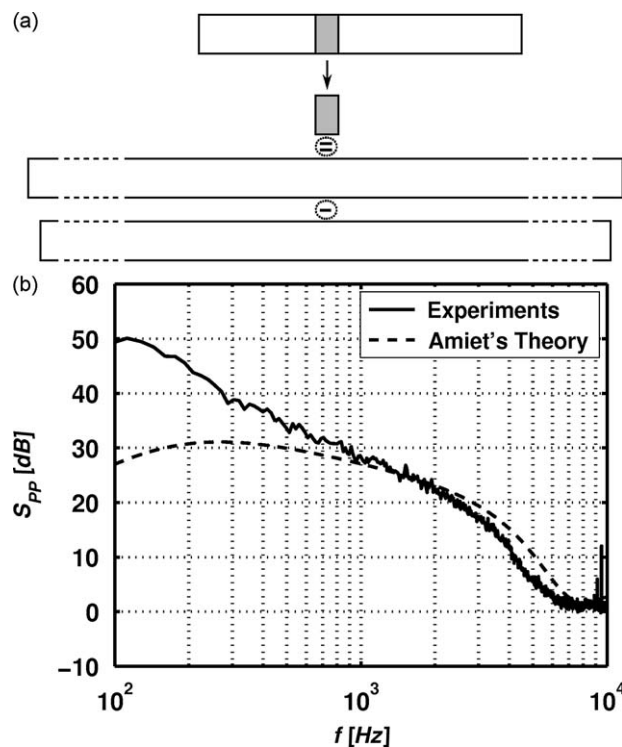


Fig. 24. Application of Amiet's theory in spanwise-varying flow conditions: (a) illustration of the inverse strip method based on the combination of large span airfoils and (b) comparison between measured sound spectra for an airfoil placed in the turbulent region of a jet and the corresponding predictions.

5.5. Progress in direct methods for computational aeroacoustics

In direct computational aeroacoustic approaches, the unsteady flow and noise fields are predicted together in a time-accurate simulation. The disparity of length scales and fluctuation amplitudes in the two fields requires numerical algorithms with broadband dispersion and dissipation relation preserving characteristics. Joint work between the AeroTraNet consortium and the University of Rome has led to the formulation of a cost-optimized prefactored compact

finite difference scheme with improved spatial and temporal resolving efficiency, applicable to shock-free acoustically active continuous flows [45]. The shorter stencil from the pre-factorization allows the use of this scheme from the second interior point inwards from the computational domain boundaries, reducing the requirement for using asymmetric or low-order stencils approaching the boundary. The optimized scheme allows 20–30 percent mesh coarsening in each spatial direction and to correspondingly increase the time step. An appropriate solid wall boundary condition enhances the monotonicity of the prediction near solid walls and prevents the onset of spurious high-wavenumber waves at this location. Whilst the pre-factorization helps towards reducing the stencil size in high-order finite difference schemes, their implementation on large distributed memory clusters requires special attention to the inter-block communication overhead introduced by the inter-block-boundary stencil size. The challenge is to develop domain decomposition and MPI code structures to obtain highly scalable high-order finite difference computational aeroacoustic schemes.

Written by Aldo Rona, ar45@leicester.ac.uk, University of Leicester, UK.

5.6. Numerical simulation of broadband combustion noise based on stochastic sound sources

The novelty of the numerical approach applied to predict broadband combustion noise lies in the stochastic reconstruction of combustion noise sources in the time domain. The highly efficient RPM-CN approach, a hybrid CFD/CAA technique, is based on a reactive flow simulation of the combustion problem. The CFD simulation can rest on a Reynolds averaged Navier–Stokes (RANS) simulation and provide statistical information of the time-averaged flow. Space–time correlations of the combustion noise sources are appropriately modelled based on statistical turbulence quantities applying the random particle-mesh (RPM) method. The stochastically reconstructed combustion noise source term is used in conjunction with the linearized Euler equations (LEE) which are integrated by the DLR's CAA-code PIANO. The accuracy

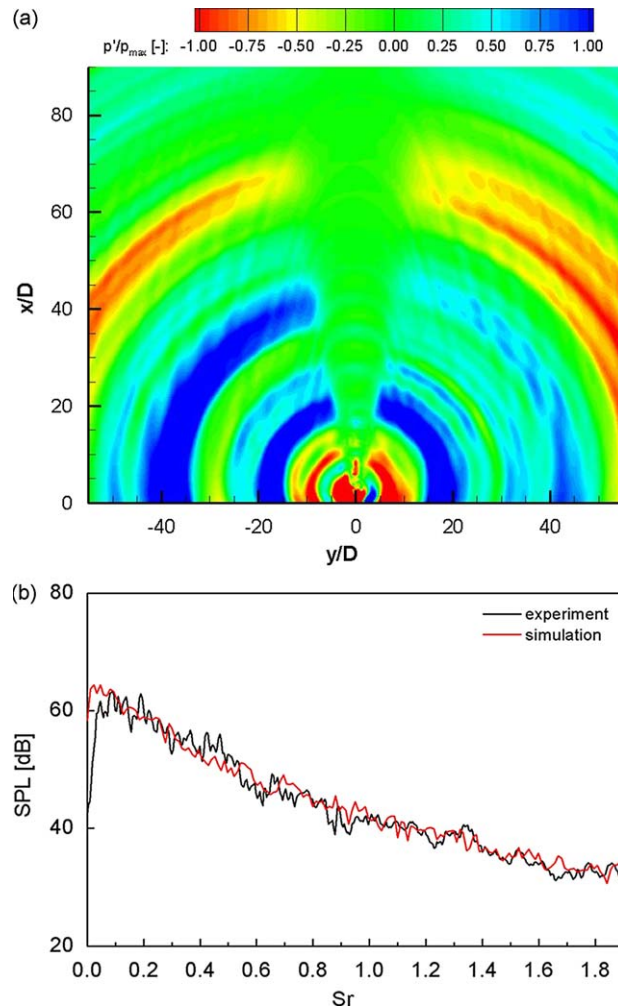


Fig. 25. Combustion noise: (a) snapshot of the calculated perturbation pressure and (b) comparison between computed sound pressure spectra and measurements for the DLR-A flame.

of the RPM-CN approach was demonstrated by a good agreement of the simulation results with acoustic measurements of the DLR-A flame. The high efficiency and therefore low computational costs enable the usage of this numerical approach in the design process. As can be seen in Fig. 25, the acoustic radiation is not omnidirectional even though the main combustion noise sources have a monopolar character. The perturbation pressure distribution displays a cone of silence, due to refraction effects induced by strong density and/or velocity gradients. The shape of the computed sound pressure level spectrum is in very good agreement with the measured one for the entire Strouhal number range (the range $0 < St < 1.9$ corresponds to $0 < f < 10,000$ Hz). The deviations of the computed sound pressure level spectrum predicted by this highly efficient numerical approach are not higher than the deviation of the spectrum predicted by high fidelity methods or statistical methods for this test case.

Written by B. Mühlbauer, bernd.muehlbauer@dlr.de, R. Ewert, O. Kornow, B. Noll, J. Delfs, M. Aigner, German Aerospace Center (DLR), Germany.

5.7. Virtual arrays for locating aeroacoustic sources on high-speed trains

Aerodynamic noise becomes a relevant source for trains running at 300 or 320 km/h. Experimental and numerical approaches are used to characterize the noise sources. A $\frac{1}{7}$ reduced scale model of a high-speed train has been characterized in a large and semi-anechoic wind tunnel (S2A: Souffleries Aéroacoustiques Automobiles) using an array of 62 microphones. The post-processing of the data takes into account the influence of the flow onto the localization and the floor reflection. The beamforming provides noise maps to localize the noise sources onto the car body. In the same time, the pressure fluctuations were computed on the surface of the car-body using a Lattice-Boltzmann method. In order to compare the experimental and numerical results, an innovative approach has been set up. A “virtual array” has been defined in the simulation and then a beamforming has been applied to the time signals provided by the simulation. Thus, a direct comparison between experiment and simulations can be easily carried out as presented in Fig. 26. This very promising approach (see details in [46]) can be improved by taking into account that the parameters of the experimental and virtual array processing are the same in this application. In practice, the virtual array offers a large number of possibilities in terms of number of microphones, array geometry, to increase the performances of the post-processing.

Written by F. Poisson, franck.poisson@sncf.fr, E. Masson, SNCF Innovation and research department, R. Gregoire, remi.gregoire@transport.als-tom.com, ALSTOM Transport, France.

5.8. Wind noise transmission into convertibles by fluid structure interaction

Since the powertrain noise and the tire-road noise of motor vehicles have been reduced continuously in the past decades, the relevance of aerodynamic noise has increased more and more [47]. In the case of convertible cars, the interior noise depends on the interaction between the aerodynamic excitation and the structure of the soft top. In cooperation with the Forschungsinstitut für Kraftfahrwesen und Fahrzeugmotoren Stuttgart and Exa Corporation a project was launched to develop a simulation technique which captures the fluid structure interaction (FSI) of a convertible soft top and the transmission of aerodynamic noise into the cabin of convertible cars. A coupling algorithm for static FSI was developed which couples Exa’s commercial CFD tool PowerFLOW and the Finite Element Solver MSC.NASTRAN. It has been shown earlier that PowerFLOW is able to predict the necessary pressure fluctuations reliably [48]. The process was used to simulate the ballooning of two test cases, of which the SAE-body (see Fig. 27a) showed strong ballooning. Fig. 27b shows

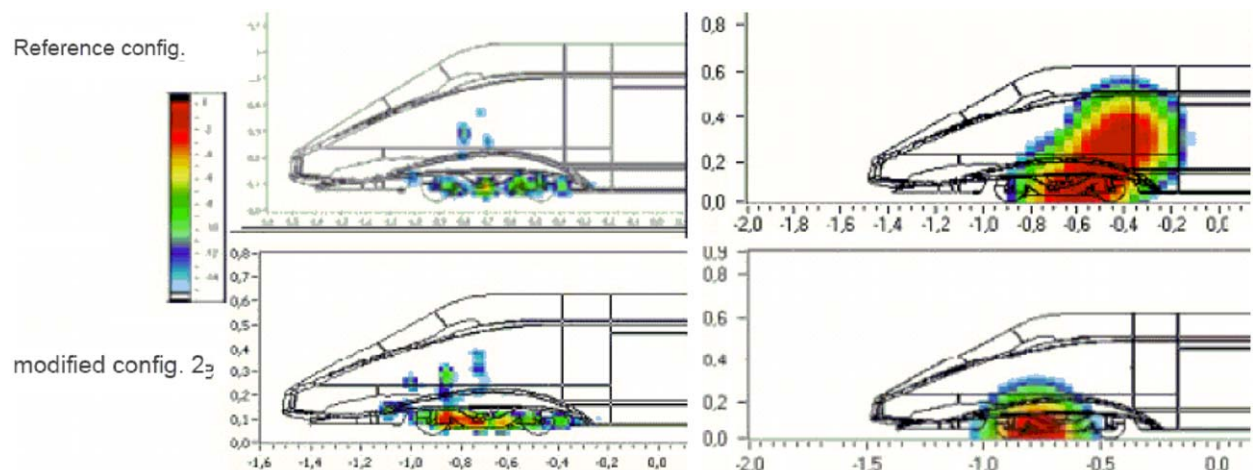


Fig. 26. Sound source localization on a high-speed train. Noise maps from the leading vehicle obtained with measured data (left part of the figure) and from computed data (right part of the figure).

the band-filtered pressure distribution on the soft top, which was already deformed by static FSI. It can be seen that strong transient effects exist. The simulation process will be extended in the near future to the transient FSI.

Written by A. Hazir, andreas.hazir@fkfs.de, R. Blumrich, Forschungsinstitut für Kraftfahrwesen und Fahrzeugmotoren Stuttgart, Stuttgart, Germany, B. Crouse and D. Freed, Exa Corp., Burlington, MA, USA.

5.9. An improved multimodal method for non-uniform lined ducts with flow and mode localized at the rigid splices

An improved multimodal method to calculate sound propagation in non-uniformly lined ducts [49] has been extended to include uniform flow and non-uniform lining. The displacement potential is expanded in terms of rigid duct modes and an additional function that carries the information about the impedance boundary. These functions are known a priori so that calculations of the true liner modes, which are difficult, are avoided. By matching the displacement potentials and axial derivatives at the interface between different uniform segments, scattering matrices are obtained for each individual segment; these are then combined to construct a global scattering matrix for multiple segments. This results in a powerful method, capable of treating many demanding configurations found in aeronautical applications (such as non-uniform lining along the azimuthal direction, high-frequencies). This method, easy to implement, is an alternative to the usual root

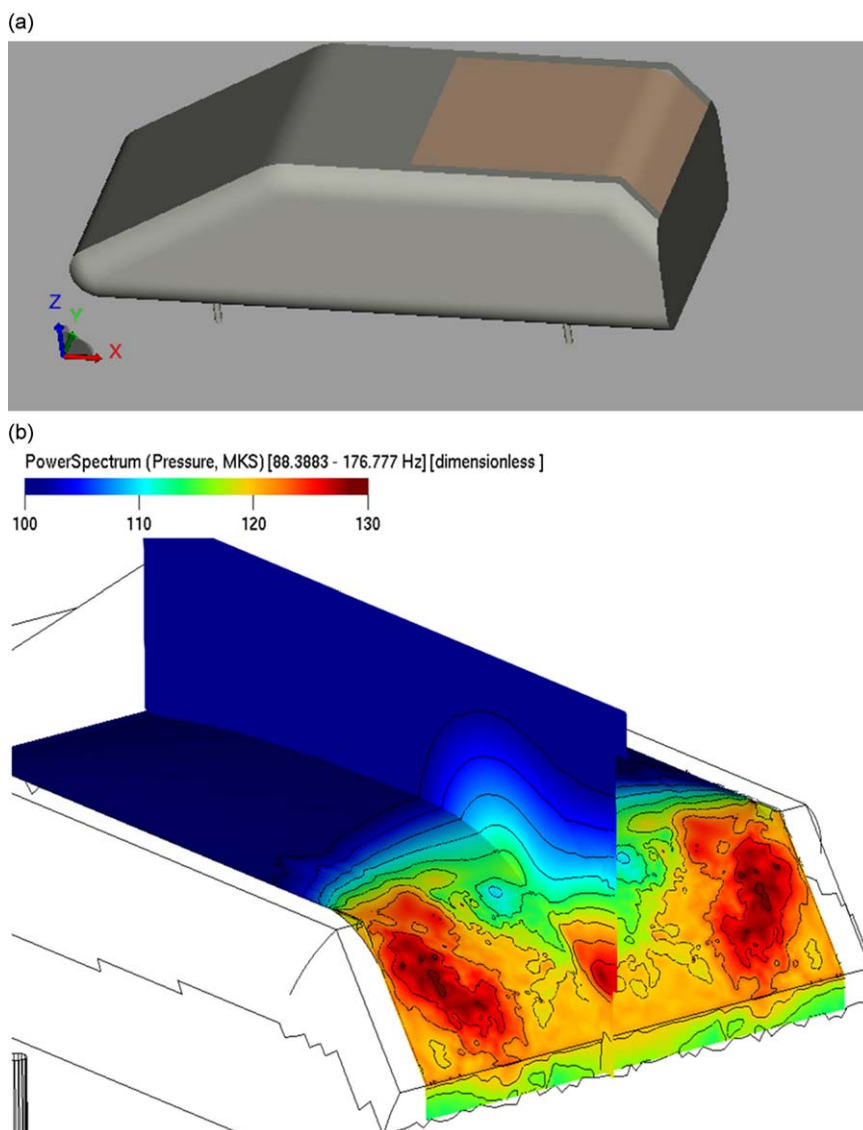


Fig. 27. Wind noise transmission into convertible cars: (a) test case for static FSI. SAE-body and (b) band filtered (88–177 Hz) static pressure on the soft top of the SAE-body.

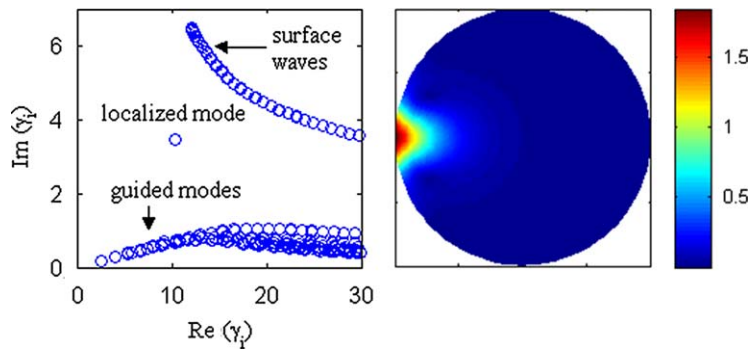


Fig. 28. Sound propagation in ducts with non-uniform lining. Appearance of a new localized mode near one splice; the eigenvalues are shown on the left part of the figure, and the eigenfunction of the localized mode is displayed on the right.

finding technique and FE method. All the modes are calculated at a time, with surface waves also well resolved. As an example, we show in Fig. 28 (left part of the figure) the calculated eigenvalues of a lined duct in the presence of a rigid splice. A new type of mode, localized in the vicinity of the rigid splice, appears [50] whose eigenfunction is also displayed in the right part of Fig. 28.

Written by Wenping Bi, wenping.bi@univ-lemans.fr, Vincent Pagneux, Denis Lafarge, Yves Aurégan, Laboratoire d'Acoustique de l'Université du Maine, France.

6. Helicopter noise

In the EU Project Friendcopter, noise abatement procedures for an EC135 have been optimized and successfully validated in flight, both by DLR. A commercial optimizer using genetic algorithms called a computation chain described in [51], able to evaluate the flyability and the ground noise of an arbitrary flight (including maneuvers), provided a data base of noise directivities for various flight conditions is available. Instantaneous noise directivity spheres were built by back-propagating the noise measured on 43 microphones during the PAVE flight tests of 2004: 4000 flight conditions including maneuver have been considered. The optimization variables are way/control points and the velocity at those points. A continuous trajectory is generated using cubic Bézier splines and provided to the Eurocopter HOST code to get the flight parameters along the trajectory. A vertical wind profile is considered. The flyability is evaluated versus safety, comfort and pilotability. All along the trajectory, adequate directivity spheres are automatically selected in the database and possibly interpolated. The SEL footprints at ground level are then calculated considering various propagation effects. The average SEL on a $6 \text{ km} \times 4 \text{ km}$ area has been minimized under flyability constraints for landing approaches starting at level flight at 100 kts, 1000 ft above the landing point and 5 km away from it. This was repeated for various helicopter masses and wind profiles. These optimizations predicted 10 dB SEL reduction under the fly path. These predictions were validated in flight tests on the EC135 FHS [52] shown by sample results in Fig. 29. A pilot display especially developed to follow noise abatement procedures has been successfully used in flight. An alternative procedure design method came from the DLR PAVE project. An analysis of the 2004 tests confirmed a suspected strong correlation between engine torque and noise on the ground. The engine torque indicator was then used to avoid a given torque range in which the noisy blade vortex interaction (BVI) occurs. A repeatable way to pilot quiet landing approaches that needs only instruments commonly on board has been defined (see [52] and bottom of Fig. 29). For both optimized and “torque-based” procedures, side-slip was used to avoid unusual Fenestron noise occurrence. Both BVI noise and Fenestron noise were then nearly unidentifiable by test observers for both procedures.

Written by Pierre Spiegel, pierre.spiegel@dlr.de, DLR Institute of Aerodynamics and Flow Technology, Braunschweig, Germany.

7. Propeller noise

7.1. CROR low-speed aerodynamic and aeroacoustic analysis

Contra rotating open rotor (CROR) propulsion systems have come back into focus as a possible economic and environmentally friendly powerplant for future transport aircraft. The DLR CFD code TAU and the FW-H-based aeroacoustic analysis tool APSIM have been employed for the analysis of the complex aerodynamics and aeroacoustics of this type of aircraft propulsion. In order to demonstrate the codes' applicability to these types of simulations, a generic 8×8 pusher CROR powerplant was designed [53] and high-fidelity URANS computations at typical sea-level take-off conditions were performed [54]. The CFD results revealed strong mutual interactions between the rotors, leading to strong periodic fluctuation of the blade loads. The dominant interaction phenomena were found to be the front rotor blade wakes and particularly the tip vortices as they interact with the aft rotor (Fig. 30a). The noise emissions are characterized by dominant

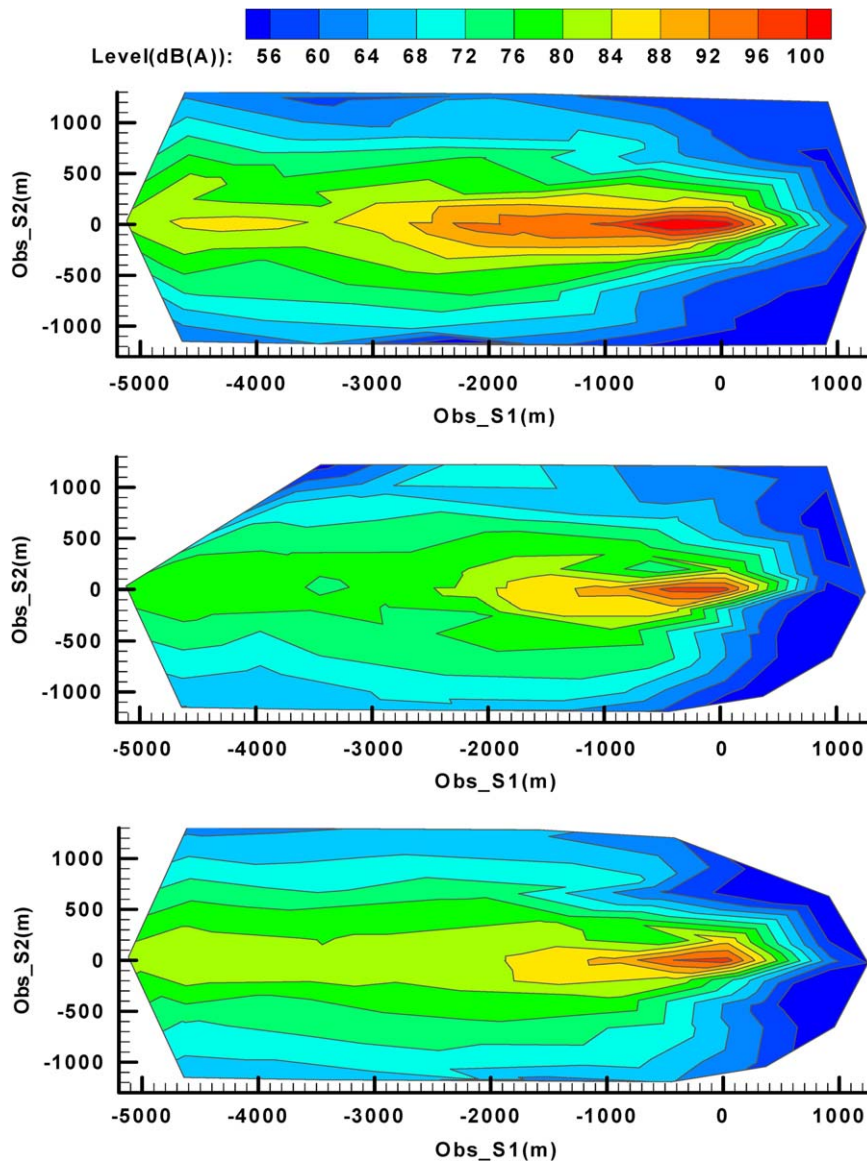


Fig. 29. Helicopter noise footprints. SEL measured at ground level on a 6×2.5 km area for EC135 landing approaches. Top: reference approach. Middle: optimized approach. Bottom: torque based approach. (10 dB noise reduction on centerline for latter both cases; noise levels are shifted by a constant value.)

rotor-alone tones in the vicinity of the planes of rotation (point a in Fig. 30b) and interaction tones radiated towards the front and rear (point b in Figs. 30b and c).

Jianping Yin, jianping.yin@dlr.de, Arne Stuermer, arne.stuermer@dlr.de, Institut für Aerodynamik und Stroemungstechnik, Braunschweig, Germany.

7.2. Multi-objective aeroacoustic optimization of an aircraft propeller

A CIRA-Piaggio Industries cooperation within the context of the European Integrated Project CESAR focussed on the aero-acoustic optimization of a Piaggio P-180 propeller configuration for a more fuel-efficient and silent aircraft. A modern software environment for multidisciplinary simulations and optimization has been used for integrating simulation tools in code networks and for applying several optimization strategies. As far as the prediction of propeller performance and noise emission is concerned, CIRA in-house numerical tools have been linked or coupled into complex numerical processes including a CSD-CFD automatic aeroelastic coupling procedure and an acoustic library implementing various surface integral formulations (e.g., porous Ffowcs Williams–Hawkings equation, Kirchhoff's method). The methodology has been used to perform a multi-objective optimization of the propeller blade shape so that the noise emission at take-off and the

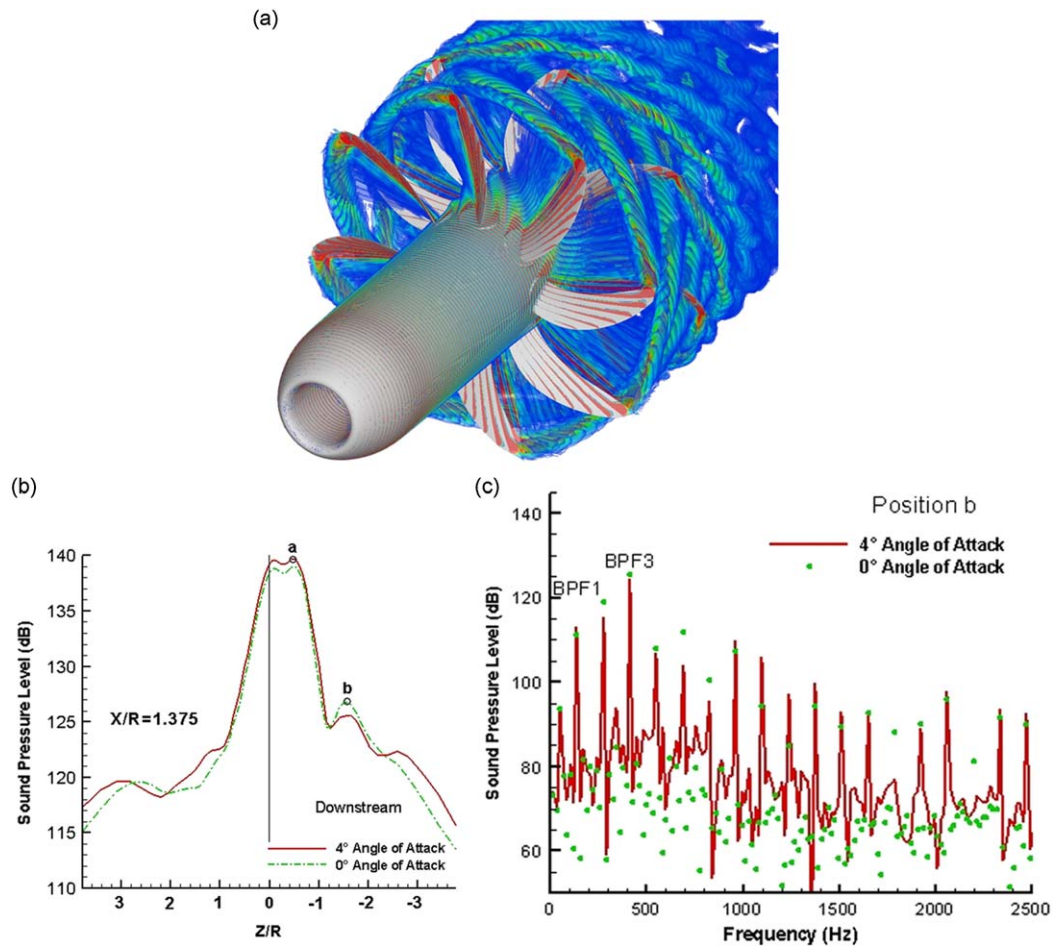


Fig. 30. Contra rotating open rotor aerodynamic and aeroacoustic analysis: (a) complex wake and vortex system, (b) near field sound pressure levels (middle) and (c) near field spectra.

efficiency in cruise have been improved while adhering to specific constraints [55,56]. Promising designs have been identified (Fig. 31a) and their noise characterization has been accomplished (Fig. 31b).

Written by A. Pagano, a.pagano@cira.it, CIRA, Italy.

8. Miscellaneous topics

8.1. Compilation and rationalization of the forms of the acoustic wave equation

The most commonly used forms of the acoustic wave equation are the classical and convected wave equations which apply to (i) linear, (ii) non-dissipative waves in, (iii) homogeneous media and (iv) at rest or in uniform motion. There are many (if not most) practical situations in which one or more of these conditions (i)–(iv) do not apply. A number of more general acoustic wave equations are available which apply to: (i) non-uniform flows, either potential or vortical, the latter including sheared and swirling mean flows; (ii) inhomogeneous and unsteady media, and also ducts of varying cross-section, i.e. horns and nozzles; (iii) nonlinear effects which can range from the second to the fourth order; (iv) dissipation by the bulk viscosity and thermal conduction and radiation. A classification of these equations is proposed in [57,58].

Written by Luis Campos, luis.campos@ist.utl.pt, IST, Portugal.

8.2. Seamless double-layer intake acoustic liner for low-thrust class turbofan engine applications

In an effort to meet severe noise attenuation and weight requirements for the small thrust class aircraft engine market sector, the Composite Research Centre (CRC) and the Engineering Department at GKN Aerospace, Cowes site, UK, have completed the first phase of a research programme aimed at developing a seamless, all-composite, double-degree of freedom, intake acoustic liner. The programme includes noise ground engine tests of selected designs. In Fig. 32, a section

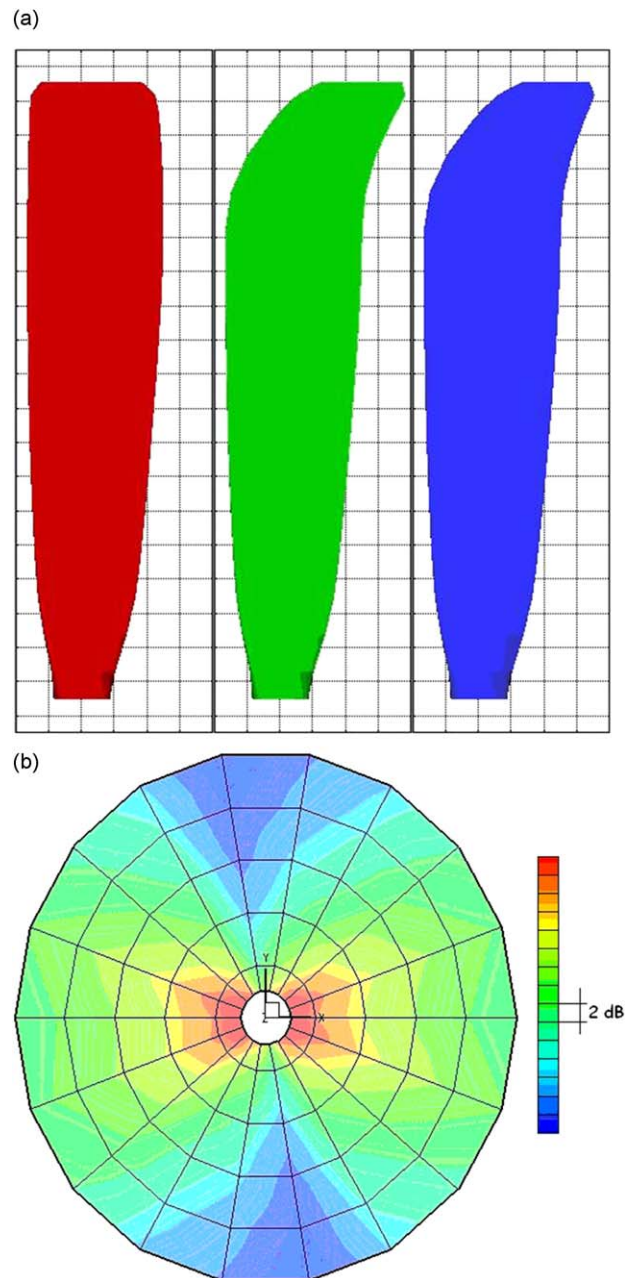


Fig. 31. Multi-objective optimization of an aircraft propeller: (a) propeller blade planforms (baseline and two optimized designs) and (b) noise directivity in the propeller plane.

of an intake acoustic liner test-piece manufactured at the CRC is shown. The primary interest of this programme is to determine the noise reduction benefits offered by a novel design incorporating a thin, cell-aligned double-layer core system, with inserted porous mesh septa, where septum DC-flow resistances properties can be effectively controlled throughout the panel. The thin core, along with the use of composite material for all the parts composing the liner, meets very stringent weight reduction targets. The static engine test data analysis shows a significant noise reduction at high power conditions over the baseline two-piece single-degree-of-freedom linear liner design, in terms of sound power levels.

Written by Armando Vavalle, GKN Aerospace, UK.



Fig. 32. Seamless double-layer intake acoustic liner.

8.3. Airbus turns to Southampton for quiet future

The Airbus Noise Technology Centre at the University of Southampton was formally launched on Monday, 3 November 2008. For many years, the University has collaborated with Airbus on a range of noise research and development projects and the new Airbus Noise Technology Centre will consolidate the relationship between the two organizations. The Center's immediate goal is to work towards the target set for the airline industry by the Advisory Council for Aeronautical Research in Europe to cut perceived noise in half by 2020 and eliminate all noise nuisance outside airport boundaries. This requires a doubling of the previous rate of progress, and requires advanced research and development across a range of new technologies. The Center, led by Professor Xin Zhang (X.Zhang1@soton.ac.uk), brings together academic staff, research fellows and PhD students using state-of-the-art computer simulations and wind tunnel testing to develop new noise reduction concepts.

Written by Kenji Takeda, ktakeda@soton.ac.uk, University of Southampton, UK.

References

- [1] S. Redonnet, G. Desquesnes, E. Manoha, Numerical study of acoustic installation effects through a chimera CAA method, AIAA Paper 2007-3501, *13th AIAA/CEAS Aeroacoustics Conference*, Roma, Italy, May 2007.
- [2] S. Redonnet, C. Parzani, E. Manoha, D. Lizarazu, Numerical study of 3D acoustic installation effects through a hybrid Euler/BEM method, AIAA Paper 2007-3500, *13th AIAA/CEAS Aeroacoustics Conference*, Roma, Italy, May 2007.
- [3] J.C. Kok, A symmetry and dispersion-relation preserving high-order scheme for aeroacoustics and aerodynamics, (NLR-TP-2006- 525), in: P. Wesseling, E. Oñate, J. Périaux (Eds.), *ECCOMAS CFD 2006*, Egmond aan Zee, The Netherlands, September 2006.
- [4] J.C. Kok, Computation of sound radiation from cylindrical ducts with jets using a high-order finite-volume method, AIAA Paper 2007-3489 (NLR-TP-2007-514), *13th AIAA/CEAS Aeroacoustics Conference*, Rome, Italy, May 2007.
- [5] S. Aéberli, NACRE Wind Tunnel Test Campaign Dedicated to New Aircraft Concepts Study, *NACRE 2nd Conference*, Greenwich, UK, 2008.
- [6] J. Ricouard, R. Davy, P. Loheac, A. Moore, O. Piccin, ROSAS Wind Tunnel Test Campaign Dedicated to Unconventional Aircraft Concepts Study, AIAA Paper 2004-2867, *10th AIAA/CEAS Aeroacoustics Conference*, Manchester, UK, May 2004.
- [7] B.J. Tester, Turbomachinery noise radiation through the engine exhaust, *Fifth Community Aeronautics Days 2006*, Vienna, Austria, June 2006.
- [8] P. Sijtsma, J. Zillmann, In-duct and far-field mode detection techniques, AIAA Paper 2007-3439, *13th AIAA/CEAS Aeroacoustics Conference*, Roma, Italy, May 2007.
- [9] P. Böhning, F. Arnold, F. Holste, M. Rose, Aerodynamic duct mode generator, AIAA Paper 2007-3433, *13th AIAA/CEAS Aeroacoustics Conference*, Roma, Italy, May 2007.
- [10] F. Arnold, U. Tapken, R. Bauers, J. Zillmann, Turbomachinery exhaust noise radiation experiments—part 1: polar directivity measurements, AIAA Paper 2008-2857, *14th CEAS AIAA Aeroacoustics Conference*, Vancouver, Canada, May 2008.
- [11] U. Tapken, R. Bauers, F. Arnold, J. Zillmann, Turbomachinery exhaust noise radiation experiments—part 2: in-duct and far-field mode analysis, AIAA Paper 2008-2858, *14th CEAS AIAA Aeroacoustics Conference*, Vancouver, Canada, May 2008.
- [12] R. Leneveu, F. Acher, S. Caro, Parallel DGM scheme for LEE applied to 3D realistic nacelle and bypass problems, AIAA Paper 2007-3510, *13th AIAA/CEAS Aeroacoustics Conference*, Roma, Italy, May 2007.
- [13] G. Gabard, B.J. Tester, L. De Mercato, Acoustic near- to far-field characteristics of nozzle radiation through plug flow jets, AIAA Paper 2007-3652, *13th AIAA/CEAS Aeroacoustics Conference*, Roma, Italy, May 2007.
- [14] R. Leneveu, B. Schiltz, S. Laldjee, S. Caro, Performance and application of discontinuous Galerkin method for turbo engine fan noise, AIAA Paper 2008-2884, *14th CEAS AIAA Aeroacoustics Conference*, Vancouver, Canada, May 2008.
- [15] Y. Ozyuruk, E. Dizemen, S. Kaya, A. Akturk, A frequency domain linearized Euler solver for turbomachinery noise propagation and radiation, AIAA Paper 2007-3521, *13th AIAA/CEAS Aeroacoustics Conference*, Roma, Italy, May 2007.
- [16] C.J. Powles, B.J. Tester, A. McAlpine, A weak scattering model for turbine tone haystacking from outside the cone of silence, *International Journal of Aeroacoustics* (2009), to appear.
- [17] C.J. Powles, B.J. Tester, Asymptotic and numerical solutions for shielding of noise sources by parallel coaxial jet flows, AIAA Paper 2008-2975, *14th CEAS AIAA Aeroacoustics Conference*, Vancouver, Canada, May 2008.
- [18] C. Haigermoser, L. Vesely, M. Novara, M. Onorato, A time-resolved particle image velocimetry investigation of a cavity flow with a thick incoming turbulent boundary layer, *Physics of Fluids* 20 (2008) 105101.

- [19] M. Grottaure, A. Rona, The radiating pressure field of a turbulent cylindrical cavity flow, AIAA paper 2008-2852, *14th CEAS AIAA Aeroacoustics Conference*, Vancouver, Canada, May 2008.
- [20] R.D. Sandberg, N.D. Sandham, Direct numerical simulation of turbulent flow past a trailing edge and the associated noise generation, *Journal of Fluid Mechanics* 596 (2008) 353–385.
- [21] R.D. Sandberg, L.E. Jones, N.D. Sandham, P.F. Joseph, Direct numerical simulations of tonal noise generated by laminar flow past airfoils, *Journal of Sound and Vibration* 320 (2009) 838–858.
- [22] R. Camussi, M. Felli, F. Pereira, G. Aloisio, A. Di Marco, Statistical properties of wall pressure fluctuations over a forward facing step, *Physics of Fluids* 20 (2008) 075113.
- [23] R. Camussi, G. Robert, M.C. Jacob, Cross-wavelet analysis of wall pressure fluctuations beneath incompressible turbulent boundary layers, *Journal of Fluid Mechanics* 617 (2008) 11–30.
- [24] S. Léwy, Prediction of turbofan rotor or stator broadband noise radiation, *Acta Acustica united with Acustica* 93 (2) (2007) 275–283.
- [25] S. Léwy, S. Heib, Prediction of rotor-stator broadband noise based on large eddy simulation, *Inter-noise 2008*, Shanghai, China, October 2008.
- [26] R. Arina, A. Iob, C. Schipani, Numerical prediction method for turbomachinery noise radiation through the engine exhaust, AIAA paper 2009-3287, *15th AIAA/CEAS Aeroacoustics Conference*, Miami, USA, May 2009.
- [27] A. Iob, R. Arina, A numerical method for the linearized Euler equations applied to turbo-machinery noise propagation through the engine exhaust, *MASCOT08-IMACS/ISGG Workshop*, Rome, 2008.
- [28] E. Gröschel, W. Schröder, P. Renze, M. Meinke, P. Comte, Noise prediction for a turbofan jet using different hybrid methods, *Computers and Fluids* 37 (4) (2008) 414–426.
- [29] S.R. Koh, W. Schröder, E. Gröschel, M. Meinke, P. Comte, Noise prediction for turbulent coaxial jets, in: C. Brun, D. Juvé, M. Manhart, C.-D. Munz (Eds.), *Notes on Numerical Fluid Mechanics and Multidisciplinary Design*, Vol. 104, Springer, Berlin, 2009, pp. 99–119.
- [30] R. Ewert, W. Schröder, Acoustic perturbation equations based on flow decomposition via source filtering, *Journal of Computational Physics* 188 (2003) 365–398.
- [31] S.A. Karabasov, M.Z. Afsar, T.P. Hynes, A.P. Dowling, W.A. McMullan, C.D. Pokora, G.J. Page, J.J. McGuirk, Using large eddy simulation within an acoustic analogy approach for jet noise modelling, AIAA Paper 2008-2985, *14th AIAA/CEAS Aeroacoustics Conference*, Vancouver, Canada, May 2008.
- [32] M.E. Goldstein, A generalized acoustic analogy, *Journal of Fluid Mechanics* 488 (2003) 315–333.
- [33] O. Power, F. Kerhervé, J. Fitzpatrick, P. Jordan, Measurements of turbulence statistics in high subsonic jets, AIAA Paper 2004-3021, *10th AIAA/CEAS Aeroacoustics Conference*, Manchester, UK, May 2004.
- [34] E. Laurendeau, P. Jordan, J.-P. Bonnet, J. Delville, P. Parnaudeau, E. Lamballais, Subsonic jet-noise reduction by fluidic control: the interaction region and the global effect, *Physics of Fluids* 20 (2008) 101519.
- [35] K.M. Eldred, Acoustic loads generated by the propulsion system, NASA SP-8072, 1971.
- [36] D. Casalino, M. Barbarino, M. Genito, V. Ferrara, Improved empirical methods for rocket noise prediction through CAA computation of elementary source fields, AIAA Paper 2008-2939, *14th AIAA/CEAS Aeroacoustics Conference*, Vancouver, Canada, May 2008.
- [37] C. Bogey, N. de Cacqueray, C. Bailly, A shock-capturing methodology based on adaptive spatial filtering for high-order non-linear computations, *Journal of Computational Physics* 228 (5) (2009) 1447–1465.
- [38] F. Grasso, S. Pirozzoli, Shock wave-vortex interaction: shock and vortex deformations, and sound production, *Theoretical and Computational Fluid Dynamics* 13 (2000) 421–456.
- [39] R. Ewert, O. Kornow, B.J. Tester, C.J. Powles, J.W. Delfs, M. Rose, Spectral broadening of jet engine turbine tones, AIAA Paper 2008-2940, *14th AIAA/CEAS Aeroacoustics Conference*, Vancouver, Canada, May 2008.
- [40] R. Ewert, Broadband slot noise predictions based on CAA and stochastic sound sources from a fast random particle mesh method (RPM), *Computers and Fluids* 37 (2008) 369–387.
- [41] S. Candel, A. Guédel, A. Julienne, Radiation, refraction, and scattering of acoustic waves in a free shear flow, AIAA Paper 76-544, 1976.
- [42] Y. Reymen, 3D High-order Discontinuous Galerkin Methods for Time-domain Simulation of Flow Noise Propagation, Ph.D. Thesis, K.U. Leuven, 2008.
- [43] T. Toulorge, W. Desmet, Curved boundary treatments for the discontinuous Galerkin method applied to aeroacoustic propagation, AIAA Paper 2009-3176, *15th AIAA/CEAS Aeroacoustics Conference*, Miami, USA, May 2009.
- [44] J. Christophe, J. Anthoine, P. Rambaud, S. Moreau, Numerical issues in the application of an Amiet model in spanwise-varying incoming turbulence, AIAA Paper 2008-2865, *14th AIAA/CEAS Aeroacoustics Conference*, Vancouver, Canada, May 2008.
- [45] A. Rona, I. Spisso, M. Bernardini, S. Pirozzoli, Comparison of optimized high-order finite-difference schemes for computational aeroacoustics, AIAA Paper 2009-0498, *47th AIAA Aerospace Science Meeting*, Orlando, USA, January 2009.
- [46] N. Paradot, E. Masson, F. Poisson, R. Grégoire, E. Guilloteau, H. Touil, P. Sagaut, Aeroacoustics methods for high speed train noise reduction, *8th World Congress on Railway Research*, Seoul Korea, May 2008.
- [47] R. Blumrich, Vehicle aeroacoustics—today and future developments, *5th International Styrian Noise, Vibration and Harshness Congress, Optimising NVH in Future Vehicles*, Graz, Austria, June 2008.
- [48] S. Senthoooran, B. Crouse, S. Noelting, D. Freed, B.D. Duncan, G. Balasubramanian, R.E. Powell, Prediction of wall pressure fluctuations on an automobile side-glass using a Lattice-Boltzmann method, AIAA Paper 2006-2559, *12th AIAA/CEAS Aeroacoustics Conference*, Cambridge, USA, May 2006.
- [49] W.P. Bi, V. Pagneux, D. Lafarge, Y. Aurégan, An improved multimodal method for sound propagation in nonuniform lined duct, *Journal of the Acoustical Society of America* 122 (2007) 280–291.
- [50] W.P. Bi, V. Pagneux, D. Lafarge, Y. Aurégan, Mode localizations at acoustically rigid splices, AIAA Paper 2009-3105, *15th AIAA/CEAS Aeroacoustics Conference*, Miami, USA, May 2009.
- [51] A. Le Duc, P. Spiegel, F. Guntzer, M. Lummer, H. Buchholz, J. Götz, Simulation of complete helicopter noise in maneuver flight using aeroacoustic flight test database, *American Helicopter Society 64th Annual Forum and Technology Display*, Montreal, Canada, April 2008.
- [52] P. Spiegel, F. Guntzer, A. Le Duc, H. Buchholz, Aeroacoustic flight test data analysis and guidelines for noise-abatement-procedure design and piloting, *34th European Rotorcraft Forum*, Liverpool, UK, September 2008.
- [53] A. Stuermer, Unsteady CFD simulations of contra-rotating propeller propulsion systems, AIAA Paper 2008-5218, *44th Joint Propulsion Conference*, Hartford, USA, 2008.
- [54] A. Stuermer, J. Yin, Aerodynamic and aeroacoustic analysis of contra-rotating propeller propulsion systems at low-speed flight conditions, *16th DGLR/STAB-Symposium*, Aachen, Germany, 2008.
- [55] A. Pagano, L. Federico, M. Barbarino, F. Guida, M. Aversano, Multi-objective aeroacoustic optimization of an aircraft propeller (CIRA-TR-08-0082), AIAA Paper 2008-6059, *12th AIAA/ISSMO Multidisciplinary Analysis and Optimization Conference*, Victoria, Canada, September 2008.
- [56] L. Federico, A. Pagano, Noise reduction and performance improvement of aircraft propellers by multi-objective optimization (CIRA-TR-08-0083), *2nd International Conference on Multidisciplinary Design Optimization and Applications*, Gijon, Spain, September 2008.
- [57] L.M.B.C. Campos, On 36 forms of the acoustic wave equation in potential flows and inhomogeneous media, *Reviews of Applied Mechanics* 60 (2007) 149–171.
- [58] L.M.B.C. Campos, On 24 forms of the acoustic wave equation in vortical flows and dissipate media, *Reviews of Applied Mechanics* 60 (2007) 291–315.